

Available online at [www.sciencedirect.com](http://www.sciencedirect.com)

**jmr&t**  
Journal of Materials Research and Technology  
journal homepage: [www.elsevier.com/locate/jmrt](http://www.elsevier.com/locate/jmrt)



## Review Article

# Additive manufacturing of polymer nanocomposites: Needs and challenges in materials, processes, and applications



Ans Al Rashid<sup>\*</sup>, Shoukat Alim Khan, Sami G. Al-Ghamdi, Muammer Koç

Division of Sustainable Development, College of Science and Engineering, Hamad Bin Khalifa University, Qatar Foundation, Education City, Doha, Qatar

### ARTICLE INFO

#### Article history:

Received 15 February 2021

Accepted 3 July 2021

Available online 9 July 2021

#### Keywords:

Additive manufacturing  
3D printing  
Polymer composites  
Nanocomposites  
Fused filament fabrication  
Powder bed fusion  
Vat photopolymerization

### ABSTRACT

Polymer nanocomposites have attracted increasing interest in research and development with several current and potential industrial applications due to their wide margin of superiority over conventional materials. Polymer composites provide a higher strength-to-weight ratio, easily customizable product properties, flexible manufacturing processes, high resistance to corrosion or erosion, and lower cost. The recent progress in additive manufacturing (AM) methods has paved the way for even a broader range of flexibilities in design and materials in several industrial sectors, including aerospace, biomedical, construction, electronics, telecommunication, mechanical, and defense. However, some hindrances remain in the synthesis of polymer composites and their fabrication through AM technologies. A comparative review of AM processes for polymer composites and their applications is presented in this study. This study aims to provide engineers and scientists with an updated understanding of the underlying issues, barriers, limitations, and opportunities. It will also help the reader to systematically reveal the research problems and future directions related to materials synthesis and AM processes.

© 2021 The Author(s). Published by Elsevier B.V. This is an open access article under the CC BY license (<http://creativecommons.org/licenses/by/4.0/>).

**Abbreviations:** Additive Manufacturing, AM; 3D Printing, 3DP; Vat Photopolymerization, VP; Digital light processing, DLP; Material Extrusion, ME; Fused Deposition Modelling, FDM; Fused Filament Fabrication, FFF; Selective laser melting, SLM; Selective laser sintering, SLS; Electron beam melting, EBM; Selective heat sintering, SHS; Multi Jet Fusion, MJF; Acoustic field-assisted projection stereolithography, A-PSL; Shape memory materials, SMM; Shape memory polymers, SMP; Polyurethane, PU; Polylactic Acid, PLA; Polycaprolactone, PCL; Polydioxanone, PDO; High-density polyethylene, HDPE; Linear low-density polyethylene, LLDPE; Acrylonitrile Butadiene Styrene, ABS; Polyamide 12, PA12; Thermoplastic Polyurethane, TPU; Polyvinylidene fluoride, PVDF; Polyethylene terephthalate, PET; Poly (methyl methacrylate), PMMA; Polystyrene, PS; Polyvinyl alcohol, PVA; Polyvinyl chloride, PVC; Waterborne polyurethane, WPU; Polyacrylonitrile, PAN; Polyimide, PI; Polyvinyl ether, PVE; Polyethylene naphthalate, PEN; Polyphenylene sulfide, PPS; Styrene-acrylonitrile resin, SAN; Cellulose Nanofibrils, CNF; Hydroxyapatite, HA; Strontium substituted HA, SrHA; Calcium carbonate, CC; Polyethylene Glycol, PEG; Graphene oxide, GO; Reduced Graphene Oxide, rGO; Functionalized graphene oxide, FGO; Carbon nanotube, CNT; Finite Element Analysis, FEA; Scanning Electron Microscopy, SEM; Coordinate Measuring Machine, CMM; Fourier Transform Infrared Spectroscopy, FTIR; Dynamic mechanical analysis, DMA; Vibrating Sample Magnetometer, VSM; Thermogravimetric analysis, TGA; X-ray Computed Tomography, XCT; Differential Scanning Calorimetry, DSC; Food and Drug Administration, FDA; Titanium dioxide, TO; Calcium copper titanate, CCT.

<sup>\*</sup> Corresponding author.

E-mail addresses: [anrashid@hbku.edu.qa](mailto:anrashid@hbku.edu.qa) (A. Al Rashid), [mkoc@hbku.edu.qa](mailto:mkoc@hbku.edu.qa) (M. Koç).

<https://doi.org/10.1016/j.jmrt.2021.07.016>

2238-7854/© 2021 The Author(s). Published by Elsevier B.V. This is an open access article under the CC BY license (<http://creativecommons.org/licenses/by/4.0/>).

## 1. Introduction

There has been an increasing need, hence a research interest, to utilize polymer composites [1]. Polymer composites provide flexibility in terms of final product properties, design, starting raw material options, and continuously expanding progressive innovations in synthesis techniques [2], in addition to their wide commercial availability and cost-effectiveness compared to other materials, such as metals and ceramics, for low-cost applications [3]. They are becoming prime choices even for critical applications (e.g., aerospace, automotive, and medical device) due to enhanced and tailored properties [4]. Polymer-based nanocomposites provide a wide margin of superiority over conventional materials due to their higher strength-to-weight ratio, easily customizable product properties, flexible manufacturing processes, and high corrosion resistance properties. Furthermore, the recent development of AM methods has provided a new production era in several industrial sectors, including biomedical, construction, electronics, telecommunication, mechanical, and defense. AM processes allow a higher degree of freedom in the design and fabrication of customized parts, rapid manufacturing, waste reduction (in some cases elimination), lower chances of human error, high precision, and accuracy at low costs [5–7].

Generally, polymers exhibit inferior mechanical, thermal, and electrical properties compared to metal and alloys for mechanical strength, thermal conductivity, and electrical conductivity, which are prime considerations for selecting materials in various applications. These properties can be improved by adding suitable additives to polymers to synthesize polymer composites of an unlimited number of kinds and properties [8]. Combining such unlimited flexibility of polymer composites with AM fabrication provides rapid, inexpensive, efficient, and multi-functional production and products [9].

Despite extensive research in synthesis and AM of polymer nanocomposites, some limitations persist, requiring further investigation. For example, particles-reinforced polymer composites face problems of inhomogeneous dispersion, inconsistent feedstock material, unlike the nature of most filler material to polymers, and little awareness of the shape and size of filler material [10]. Resolution, repeatability, and printability need to be enhanced by optimizing AM process conditions and starting material parameters together [11]. Finally, interfacial interaction/bonding, the material's composition, and structural defects need to be analyzed in detail to ensure excellent product performance.

In this article, the authors present an up-to-date review of polymer nanocomposites, their manufacturing potentials, issues, and opportunities using AM (also widely known as 3D printing- 3DP) technologies and their applications in different sectors. Building upon a comprehensive and comparative review and analysis of various research papers and existing reviews, this study's main aim is to provide researchers with topical hindrances and limitations in AM of these materials. This paper will provide a concise guideline to engineers, scientists, and technologists from various industrial sectors to select the most appropriate materials, synthesis techniques,

and AM process options for their targeted application. An extensive discussion is presented to address these processes' restrictions, from material synthesis to characterization of final AM components. This study's objectives include discussing limitations related to the synthesis of polymer nanocomposites, research gaps to avoid AM process constraints, factors affecting the end-product performance in 3D printed polymer nanocomposites, and presentation of research directions to achieve effective and sustainable materials & processes.

This literature review is performed using the following methodology. The overall goal was to have a broad understanding and detailed analysis of additive manufacturing (AM)/3D printing (3DP) of polymer matrix nanocomposite materials. For this purpose, different databases (Scopus, Web of Science, Springer, and Wiley) were accessed to acquire the research articles within the study's scope. The search for articles was performed using different keywords (additive manufacturing, 3DP, polymer, nanocomposite) to consider as much relevant literature as possible. Then, articles containing searched terminologies in title, abstract, and keywords were filtered and investigated thoroughly for further reading and review. To further specify the article's scope within polymer nanocomposites, studies comprising fiber-reinforced composite materials were not considered for this review. Therefore, studies related to nanoparticle reinforced composites are presented. As fiber-reinforced composites and their AM itself is an independent topic, limitations and processes are different; therefore, it would require a separate study to deliver it.

The first section discusses the use of different AM processes, working principles, materials, advantages, and limitations. The second section presents the recent advances on AM of polymer nanocomposites, and the following section includes the industrial applications of 3D printed polymer nanocomposites in various industrial sectors. Finally, a critical analysis of reviewed articles was performed to identify challenges related to AM of polymer nanocomposites with a detailed discussion on future research directions addressing the gaps identified in the literature.

## 2. Additive manufacturing (AM) processes

Several AM processes currently exist, which have been utilized for rapid prototyping applications. Depending upon the working principles, AM processes can be broadly classified into seven categories, vat polymerization (VP), powder bed fusion (PBF), material extrusion (ME), material jetting (MJ), binder jetting (BJ), directed energy deposition (DED), and sheet lamination (SL) [12]. Generally, AM technologies use computer-aided design (CAD) models [13]. Cross-sections of the geometries are defined from these CAD models, and material is added to each layer to make a tangible and intricate part. This review mainly focuses on three AM techniques: vat polymerization, powder bed fusion, and material extrusion, as these processes are most widely utilized for polymer nanocomposites. Plenty of materials have been developed for each AM process commercially available with AM technologies in the market. Following, we present the working principles of

**Table 1 – Comparison of AM Processes considered for this study.**

AM Process	Feedstock Type	Materials	Resolution ( $\mu\text{m}$ )	Advantages	Limitations
Vat Polymerization	Liquid	Photopolymers	25	<ul style="list-style-type: none"> <li>- Highest resolution among mentioned processes.</li> </ul>	<ul style="list-style-type: none"> <li>- Slow process due to curing</li> <li>- Refill intervals add delays</li> <li>- Poor mechanical properties due to insufficient polymerization and curing</li> </ul>
Material Extrusion	Solid (Filament)	Thermoplastics	50–500	<ul style="list-style-type: none"> <li>- Cheap technology</li> <li>- Most widely available commercially.</li> <li>- Can process both amorphous and crystalline polymers.</li> </ul>	<ul style="list-style-type: none"> <li>- Relatively lower resolution.</li> <li>- Lower mechanical properties compared to injection molded parts.</li> <li>- High porosity.</li> <li>- Difficult control of numerous process parameters involved.</li> </ul>
Powder Bed Fusion	Powder	Thermoplastics, Metals, Glass, Ceramics	60–150	<ul style="list-style-type: none"> <li>- No support material required.</li> <li>- Recycling of unused material.</li> <li>- Capability to produce very complex parts.</li> <li>- Higher structural integrity.</li> </ul>	<ul style="list-style-type: none"> <li>- As-built parts exhibit poor surface finish, dimensions, and mechanical properties.</li> <li>- Requires post-processing treatments (surface polishing, heat treatments)</li> </ul>

selected AM processes and related benefits and limitations for each technology. Table 1 shows the comparison of different AM processes considered for this study.

### 2.1. Vat photopolymerization (VP)

The vat photopolymerization process is an AM technique in which photo-sensitive materials are exposed to radiation/light in a controlled manner to obtain polymerized material layers. Subsequent layers combine to form a 3D object; however, this process's application is limited to the materials that polymerize on exposure to light [14]. Photopolymers and resins can be processed using this technology [15]. Depending upon the variation in curing source, VP processes can further be classified into; Stereolithography (SLA), digital light processing (DLP), two-photon polymerization (2PP), and volumetric 3D printing [16].

SLA photopolymer resins mainly consist of monomers, oligomers/binders, photoinitiators, and some additives. Monomers and oligomers are the main constituents of photopolymer resin, which solidifies due to crosslinking. Photoinitiators convert into radicals and react with oligomers and monomers, providing crosslinking to produce polymer chains on exposure to curing light. Additives may include nanoparticles or pigmentation for improved resin properties or desired coloring [17].

Digital light processing (DLP) also relies on UV light-induced polymerization of the resin [4]. The significant difference between these two technologies resides in that DLP induces an instantaneous entire layer polymerization using digital micro-mirrors devices (DMD) [18,19]. In contrast, in SLA, a single laser point (e.g., layer pixel) is exposed at a time. As a result, DLP offers a higher printing speed than SLA and other technology competitors [20]. The applied light source has also evolved from standard lamps to light-emitting diode covering, thus, a more comprehensive range of wavelengths at a lower cost [21]. The hardware setup for DLP offers higher lateral printing resolution. The z-resolution is tightly correlated with light penetration and scattering, which can be improved by adding light absorbers and polymerization facilitators. DLP achieves a resolution of about  $1 \mu\text{m}$  (while the printing speed is about  $30\text{mm}^3 \text{ s}^{-1}$ ) regardless of the layer's lateral area and complexity [22]. The working principles of SLA and DLP technologies are presented in Fig. 1.

Two-photon polymerization (2PP) is another vat polymerization-based printing system like SLA and DLP, but it can provide better control and higher print quality [23]. Due to single-photon polymerization in SLA, the process occurs on the surface of a photosensitive resin that only allows building 3D structures layer by layer. On the other hand, in 2PP, which uses near-infrared (NIR) femtosecond (Fs) laser pulses, the two photons are simultaneously absorbed by the

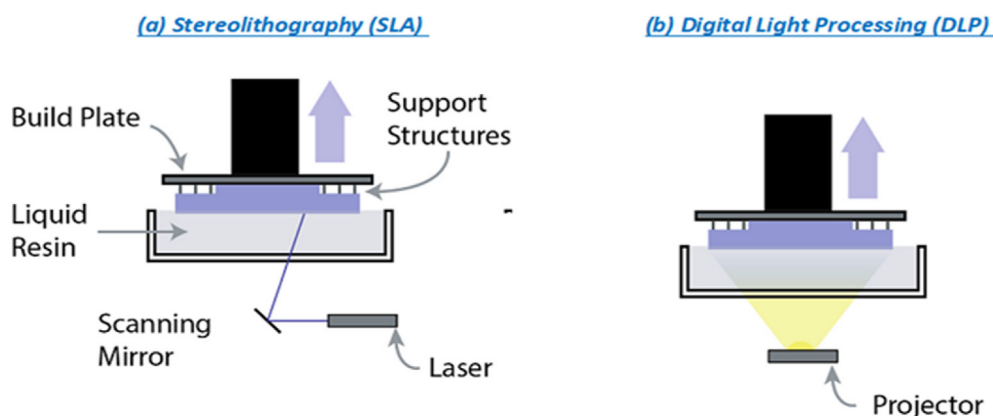


Fig. 1 – Working principle of (a) SLA and (b) DLP technologies (reproduced with permission from [4]).

photo-initiator [4]. Allowing them to act as a single photon to initiate polymerization, enabling direct writing of any desired 3D model into the volume of photosensitive materials transparent in the NIR and highly absorptive in the UV spectral range [24].

Volumetric 3D printing directly prints structures in three dimensions by using a rotating vat and an index-matching resin [25]. Projecting six distinct images of the object taken from specific angles and continuously alternating them during rotation allows objects to be built. Contrary to other methods where the 3D structure is built by 2D layers, the object is created directly in 3D [16,26].

VP processes provide the highest printing resolution among the processes discussed here. Despite having an excellent resolution, several factors affect the properties of 3D-printed parts. The main limitation is the printing time; although the technology can quickly produce one layer, curing the processed layer takes time. Secondly, the resin needs to be refilled continuously in the resin tank, which adds delays to the process. Finally, the mechanical properties of the 3D printed parts are affected by the degree of polymerization and post-print curing process [27].

## 2.2. Material extrusion (ME)

In extrusion-based processes, the semi-solid liquid is extruded on a build surface through a nozzle, solidifying in an extruded shape, with further layers extruded sequentially to obtain a solid part [12]. The most commonly used technique under this category is fused filament fabrication (FFF), also known as fused deposition modeling (FDM). In the FFF process, the material is supplied in the form of filaments. It is heated in a heating chamber to attain the required viscosity and extruded through a nozzle over a platform [13]. FFF sales in 2016 shared 96% of the global AM market; therefore, it is the most widely used AM technology [28]. Thermoplastics, metal particles reinforced polymers, and hydrogels have been fabricated using extrusion processes [29]. Generally, the feedstock material in FFF is provided in the form of a filament spool. A mechanism of roller and gear is used to feed filament material into a heating chamber, which heats and deposits the material onto the

build platform (Fig. 2). FFF 3D printers may have dual extruders to allow multi-material fabrication or 3D fabricate support structures for overhanging structures [30].

Significant bonding between adjacent extruded filaments is vital to achieving the desired strength through the intermolecular interaction of polymer chains. Turner et al. [31] investigated this phenomenon and concluded that several parameters govern this polymer fusion, including viscosity, thermal conductivity, heat capacity, and cooling rate. Interlaminar adhesion is another critical issue related to FFF processes, as fabricated parts can undergo delamination under shear forces due to insignificant adhesion between the layers [32]. Process parameters in FFF can be categorized into three categories: slicing, building orientation, and temperature conditions (Fig. 3), as defined by Popescu et al. [33]. The print quality and mechanical properties of parts fabricated through the FFF process also depend upon several parameters, as shown in Fig. 4.

The prime advantage of this AM technology over others is its lower price and its broad commercialization [10]. Although the printing resolution is lower, different amorphous and crystalline materials can be processed using the

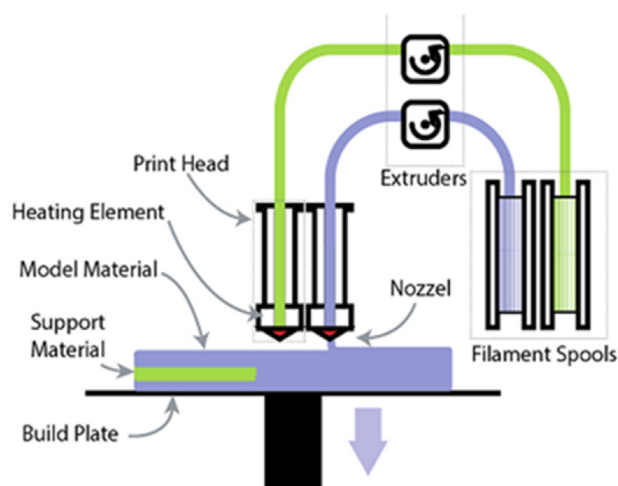


Fig. 2 – Working principle of fused filament fabrication technology (reproduced with permission from [4]).

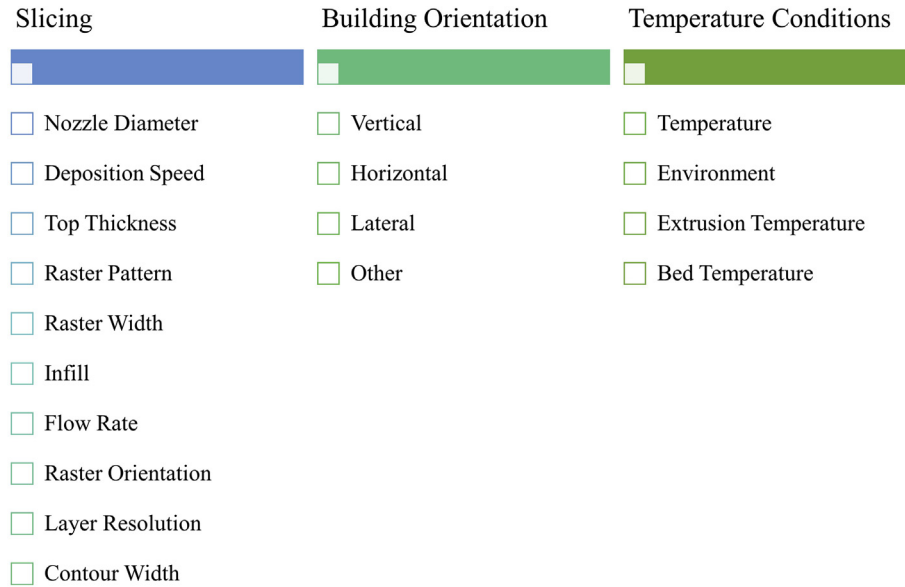


Fig. 3 – Process parameters for FFF process [33,34].

FFF technique. Despite having plenty of advantages over other processes, the main limitation is the inferior mechanical properties compared to injection molded parts due to anisotropy and high porosity [36]. Optimization of process parameters involved in this process is an active research interest, as various parameters affect final product performance.

2.3. Powder bed fusion (PBF)

In powder bed fusion processes, the powdered material is carried in a bed, and a layer of material is solidified using a heat source. Once the fusion of one layer is performed, a new layer of powdered material is added for the subsequent layer [12]. Different heat sources are utilized to perform the melting

or sintering process of powder. Selective laser melting (SLM) and selective laser sintering (SLS) processes utilize the laser source, an electron beam is used in electron beam melting (EBM), and a thermal printhead performs the function of material sintering in the selective heat sintering (SHS) process [37]. PBF processes provide higher resolutions compared to extrusion-based techniques. Polymer powders, metal alloys, and ceramics can be processed using these processes [38].

SLS is the most widely used PBF process, in which 3D objects are fabricated using powder material in a layer-by-layer manner. Thermal energy (focused laser radiations) selectively fuses the material depending upon the design of the fabricated object [39]. SLM process differs from SLS in terms of solidification of material and resulting bonding mechanisms. SLM process relies on the melting of the

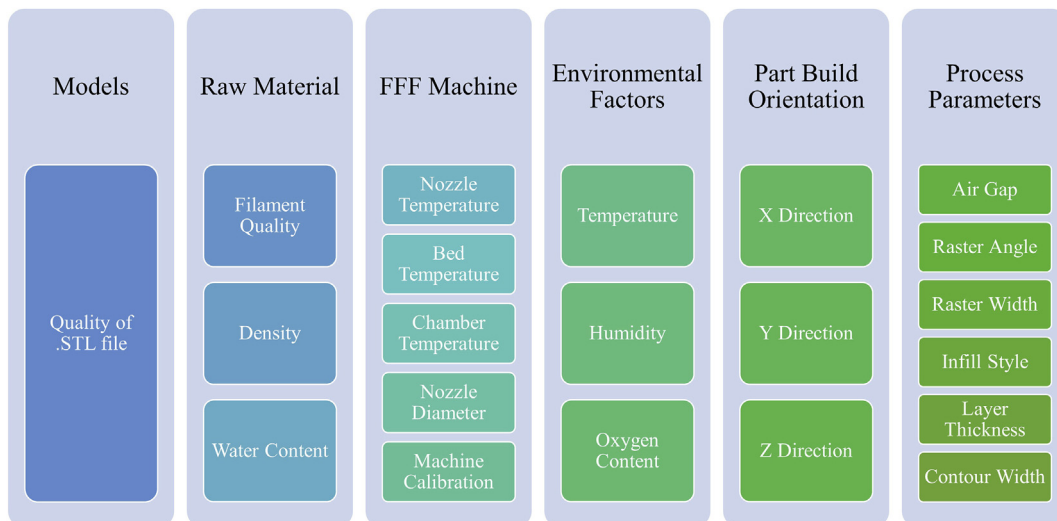


Fig. 4 – Factors affecting Print Quality and Mechanical Performance in FFF Process [35].

**Table 2 – Highlights on 3D printed polymer nanocomposites.**

Material	Reinforcement (wt%)	AMP	Synthesis Technique	Improved Properties/Applications	Ref.
PLA	HA (5–30%)	FFF	Sol–gel	<ul style="list-style-type: none"> <li>• Biomedical implants</li> <li>• Compressive strength: 19%</li> <li>• Flexural strength: 9.5%</li> <li>• Impact strength: 30%</li> <li>• Loading cycles: 14%</li> </ul>	[57]
PLA	HA (5–15%)	FFF	Solution Mixing	<ul style="list-style-type: none"> <li>• Synthetic trabecular bone</li> <li>• Enhanced mechanical properties</li> <li>• Comparable strength of the full-scale specimen</li> </ul>	[58]
PLA	HA (5–25%)	FFF	Melt Blending	<ul style="list-style-type: none"> <li>• Medical applications</li> <li>• Thermomechanical: 12%</li> <li>• Increase in cell proliferation</li> </ul>	[59]
PLA	Carbon Black	FFF	–	<ul style="list-style-type: none"> <li>• Low Voltage applications</li> <li>• Improved mechanical strength as compared to conventional materials</li> </ul>	[61]
PLA	CNT	FFF	Melt Blending	<ul style="list-style-type: none"> <li>• Electro-conductive Applications</li> </ul>	[62]
PLA	CNF (10–40%)	FFF	Solution Mixing	<ul style="list-style-type: none"> <li>• Mechanical engineering</li> <li>• Tensile strength: 80%</li> <li>• Elastic modulus: 200%</li> <li>• Strain at break: 76%</li> <li>• Toughness: 220%</li> </ul>	[64]
PLA	CNT	FFF	–	<ul style="list-style-type: none"> <li>• Shape memory applications</li> <li>• Recovery force: 144%</li> <li>• Shape memory ratio: 97.3%</li> <li>• Peak load: 28.5–60.2%</li> </ul>	[63]
PLA	Cloisite 30B (Nanoclay)	FFF	–	<ul style="list-style-type: none"> <li>• Increased dynamic mechanical properties</li> </ul>	[60]
PLA	rGO	FFF	Melt Blending	<ul style="list-style-type: none"> <li>• Better shape stability</li> <li>• Electrical applications</li> <li>• Improved electrical conductivity</li> <li>• Percolation threshold: between 4 and 8 wt%</li> <li>• Electrical conductivity: 476 S/m at 6wt% content</li> </ul>	[65]
PCL	HA/SrHA (0–20%)	ME	Mechanical Mixing	<ul style="list-style-type: none"> <li>• Bone Tissue Engineering</li> <li>• Improved mineralization</li> <li>• Significant biocompatibility</li> <li>• Substantial cell proliferation</li> </ul>	[68]
HDPE	Cardboard Dust (20–75%)	FFF	Mechanical Mixing	<ul style="list-style-type: none"> <li>• Low-Cost Structures</li> <li>• Damping capacity</li> <li>• Low plastic deformation</li> </ul>	[70]
HDPE	CNT	FFF	Melt Blending	<ul style="list-style-type: none"> <li>• Electro-conductive Applications</li> </ul>	[62]
ABS	Metallic particles	FFF	Solution Mixing	<ul style="list-style-type: none"> <li>• Aeronautics and aerospace</li> <li>• High filling ratio of metallic particles</li> <li>• Tuned number of particles and physical properties</li> </ul>	[71]
ABS	ZnFe <sub>2</sub> O <sub>4</sub> (0–14%)	FFF	Solution Mixing	<ul style="list-style-type: none"> <li>• Low electrical conductivity applications</li> <li>• Tensile strength: 52%</li> <li>• Hardness: 75%</li> <li>• Thermal conductivity: 87%</li> </ul>	[74]
ABS	Montmorillonite (MMT)	FFF	Melt Blending	<ul style="list-style-type: none"> <li>• Thermal and Mechanical</li> <li>• Improved tensile strength &amp; elastic modulus</li> <li>• Lower thermal expansion ratio</li> <li>• Higher thermal stability</li> </ul>	[54]
ABS	OMMT	FFF	Solution Mixing	<ul style="list-style-type: none"> <li>• Microwave &amp; Radio Frequency components</li> </ul>	[49]
ABS	MMT, MWCNT, CaCO <sub>3</sub> , SiO <sub>2</sub>	FFF	Melt Blending	<ul style="list-style-type: none"> <li>• Improved mechanical properties</li> <li>• Improved tensile and flexural strength</li> <li>• CaCO<sub>3</sub> provided highest failure strain</li> <li>• Reduced anisotropic effect with CaCO<sub>3</sub> reinforcement</li> </ul>	[47]

(continued on next page)

Table 2 – (continued)

Material	Reinforcement (wt%)	AMP	Synthesis Technique	Improved Properties/Applications	Ref.
ABS	MWCNT (1–15%)	FFF	Melt Blending	<ul style="list-style-type: none"> <li>• Electrical, mechanical and thermal applications</li> <li>• Reduced melt flow index</li> <li>• Improved electrical and thermal conductivity</li> </ul>	[76]
ABS	MWCNT (0–8%)	FFF	Melt Blending	<ul style="list-style-type: none"> <li>• Improved elastic modulus and strength</li> <li>• Electrical and mechanical applications</li> <li>• Reduced melt flow index</li> <li>• Improved mechanical and electrical properties</li> <li>• Optimum properties at 6% concentration</li> </ul>	[77]
ABS	rGO	FFF	Solution Mixing	<ul style="list-style-type: none"> <li>• Electrical applications</li> <li>• Better dispersion due to functional groups</li> <li>• Improved electrical conductivity</li> </ul>	[114]
ABS	Graphene (2–8%)	FFF	Melt Blending	<ul style="list-style-type: none"> <li>• Mechanical applications</li> <li>• Improved elastic modulus</li> <li>• Optimum graphene content: 4 wt%</li> </ul>	[53]
ABS	GO (0.02–0.06)	FFF	Solution Mixing	<ul style="list-style-type: none"> <li>• Mechanical applications</li> <li>• Improved strength and stiffness</li> <li>• Maximum properties improvement at 0.06 wt% GO</li> <li>• Failure strain: 29%</li> <li>• Toughness: 55%</li> </ul>	[78]
PVDF	Zirconium tungstate (1–10%)	FFF	Melt Blending	<ul style="list-style-type: none"> <li>• Mechanical engineering</li> <li>• Low coefficient of thermal expansion</li> <li>• Improved printability</li> <li>• Enhanced dimensional tolerances</li> </ul>	[79]
PVDF	MWCNT/BT	FFF	Melt Blending	<ul style="list-style-type: none"> <li>• Energy harvesting &amp; pressure sensors</li> <li>• Improved piezoelectric conversion efficiency</li> <li>• Piezoelectric coefficient upto: 129 pC/N</li> <li>• Simplified sensor manufacturing</li> </ul>	[50]
TPU	MWCNT (1–5%)	FFF	Melt Blending	<ul style="list-style-type: none"> <li>• High Strain Sensors</li> <li>• Improved interlayer adhesion and elastic modulus</li> <li>• Consistent piezoresistive response</li> </ul>	[51]
TPU	MWCNT (1–2%)	FFF	Melt Blending	<ul style="list-style-type: none"> <li>• Mechanical Applications</li> <li>• Improved elastic modulus</li> <li>• Higher tensile strength for axial printing direction</li> </ul>	[82]
PBT	CNT, Graphene	FFF	Solution Mixing	<ul style="list-style-type: none"> <li>• Electrical applications</li> <li>• Percolation threshold at: 0.49 wt% for CNT</li> <li>• Percolation threshold at: 5.2 wt% for Graphene</li> </ul>	[83]
Epoxy	CNF - PEG treated (1–5%)	VP	Melt Blending	<ul style="list-style-type: none"> <li>• Mechanical engineering</li> <li>• Tensile strength: 24%</li> <li>• Hardness: 82%</li> </ul>	[98]
Epoxy	CNF - rGO treated (1–10%)	VP	Melt Blending	<ul style="list-style-type: none"> <li>• Mechanical engineering</li> <li>• Tensile strength: 37%</li> <li>• Hardness: 129%</li> </ul>	[98]
Photopolymer	SrFe <sub>12</sub> O <sub>19</sub> (5%)	VP	Mechanical Mixing	<ul style="list-style-type: none"> <li>• Electrical &amp; electronics</li> <li>• Stable particle suspension</li> <li>• Improved yield point &amp; viscosity</li> </ul>	[101]
Photopolymer	TO or CCT (5–20%)	VP	Mechanical Mixing	<ul style="list-style-type: none"> <li>• Electromagnetic elements</li> <li>• Improved viscosity, shear rate &amp; dielectric permittivity</li> </ul>	[103]

**Table 2 – (continued)**

Material	Reinforcement (wt%)	AMP	Synthesis Technique	Improved Properties/Applications	Ref.
Photopolymer	Nanosilica (1–15%)	DLP	Mechanical Mixing	<ul style="list-style-type: none"> <li>• Shape memory materials</li> <li>• Curing: From 4s to 0.7s</li> <li>• Tensile Strength: 2.4–3.6x</li> <li>• Shape fixity: 100%</li> <li>• Shape recovery: 90–97%</li> </ul>	[104]
Photopolymer (UV 6105)	MMT (Dellite 43B)	SLA	Mechanical Mixing	<ul style="list-style-type: none"> <li>• Mechanical applications</li> <li>• Improved reactivity 15% at 0.3 wt% loading</li> <li>• Diffusion aid by particles in polymerization process</li> </ul>	[99]
Photopolymer	MMT & Attapulgate	SLA	–	<ul style="list-style-type: none"> <li>• Mechanical applications</li> <li>• Improved tensile modulus for both nano-clays</li> <li>• Improved elastic strength for MMT</li> </ul>	[100]
PCL/PDO	–	FFF	Solution Mixing	<ul style="list-style-type: none"> <li>• Gastrointestinal Stents</li> <li>• Beneficial for cell growth</li> <li>• Safe during interaction with blood</li> </ul>	[107]
PLA/TPU	–	FFF	Melt Blending	<ul style="list-style-type: none"> <li>• 4D Printing</li> <li>• Low-cost shape memory material</li> <li>• Decent shape memory and shape fixity characteristics</li> </ul>	[108]
TPU/PLA	GO	FFF	–	<ul style="list-style-type: none"> <li>• Mechanical &amp; biomedical applications</li> <li>• 75.5% increase in elastic modulus</li> <li>• 69.2% increase in tensile strength</li> <li>• Assisted cell growth</li> </ul>	[110]
Epoxy	Magnetite (55–75%)	DIW	Mechanical Mixing	<ul style="list-style-type: none"> <li>• EM radiation shielding or thermal applications</li> <li>• Improved compressive strength and ductility</li> </ul>	[106]
PA12	Graphene	FFF	–	<ul style="list-style-type: none"> <li>• Mechanical applications</li> <li>• Lower crystallinity</li> <li>• Improved thermal stability</li> </ul>	[86]
PA12	Glass beads (40%)	MJF	Melt Blending	<ul style="list-style-type: none"> <li>• Mechanical engineering</li> <li>• Tensile modulus: 85%</li> <li>• Flexural modulus: 36%</li> <li>• Porosity: &lt;1%</li> </ul>	[87]
PA 12	Carbon Black	SLS	–	<ul style="list-style-type: none"> <li>• Electrical and Electronics applications</li> <li>• Improved electrical conductivity</li> <li>• Low percolation threshold</li> </ul>	[89]
PA12	MWCNT	SLS	–	<ul style="list-style-type: none"> <li>• Mechanical applications</li> <li>• Improved tensile strength: 10%</li> </ul>	[90]
PA12	Carbon Nanofibers	SLS	–	<ul style="list-style-type: none"> <li>• Mechanical applications</li> <li>• Improves storage modulus: 22%</li> </ul>	[91]
PA11 & PA12	MMT, CNF, MWCNT	SLS	–	<ul style="list-style-type: none"> <li>• Mechanical applications</li> <li>• Improved thermal and mechanical properties</li> <li>• Enhanced flame retardancy</li> <li>• Reduced flammability</li> </ul>	[92–94]
PA12	Nanosilica	SLS	–	<ul style="list-style-type: none"> <li>• Thermal and mechanical applications</li> <li>• Tensile strength: 20.9%</li> <li>• Tensile modulus: 39.4%</li> <li>• Impact strength: 9.54%</li> </ul>	[88]
PLA	CC (25%)	SLS	Mechanical Mixing	<ul style="list-style-type: none"> <li>• Bone Tissue Engineering</li> <li>• Strength up to 75 MPa</li> <li>• Good biocompatibility</li> </ul>	[66]

powdered material to the liquid phase; however, in SLS, partial liquefaction is practiced [40]. Different laser sources are implemented depending upon the absorptivity of the powder material [41]. CO<sub>2</sub>, Nd:YAG, short-pulse Cu-vapor, and fiber laser are the most widely reported thermal energy sources for SLS [42].

PBF processes do not require to build support material, as the unsintered powder material acts as support material to complex or overhanging structures [43]. Besides, this material can be recycled for use in the fabrication of parts without significant changes in properties. The major drawback of these processes is post-processing treatments for better



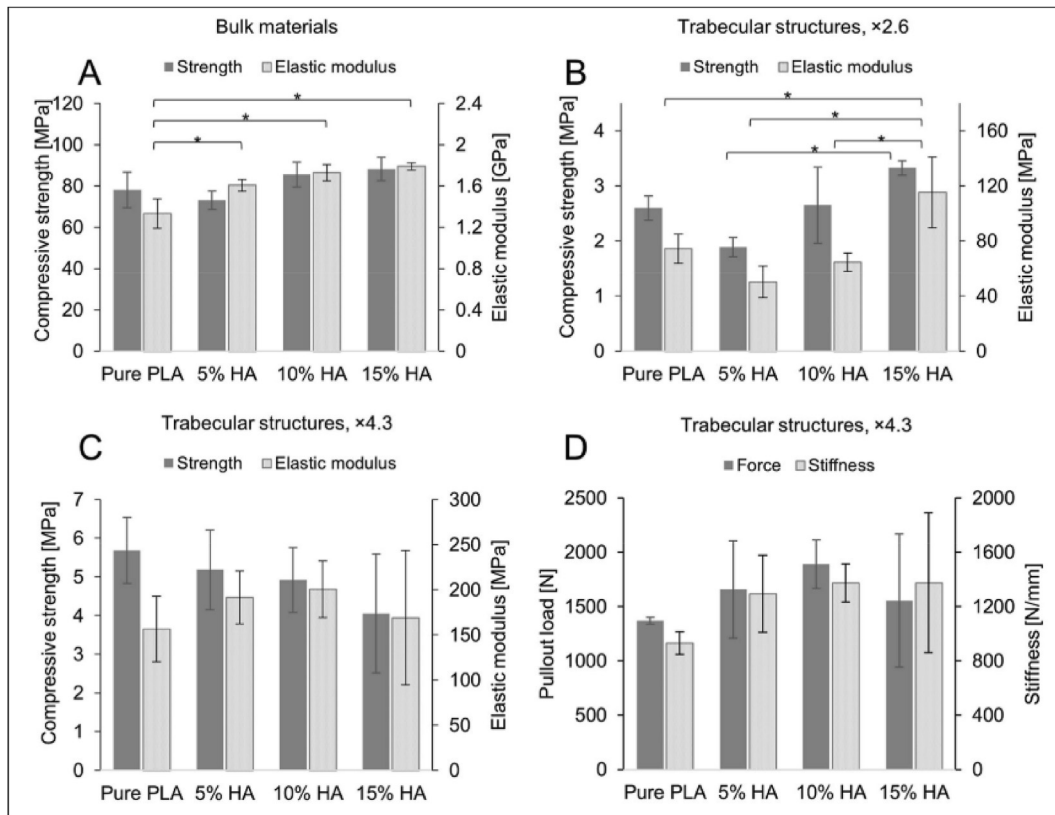


**Fig. 5 – Compressive Strength & Elastic Modulus of PLA/HA Nanocomposites (A) Bulk Materials (B) x2.6 Trabecular Model (C) x4.3 Trabecular Model (D) Pullout Force & Stiffness of x4.3 Trabecular Model (Reproduced with Permission from [58]).**

surface finish and heat-treatments for improved mechanical properties [44].

### 3. Additive manufacturing of polymer nanocomposites

The commercially available polymers for AM cannot perform adequately in high-performance applications. Therefore, it is vital to synthesize functional polymer materials compatible with AM processes discussed above. Generally, polymers do not exhibit significant mechanical, thermal, and electrical properties as they do not demonstrate substantial strength, heat transfer capabilities, and conductivity. Therefore, they are altered by introducing filler particles or reinforcement to achieve desired properties for functional applications.

Polymer nanocomposites are obtained by adding nanofillers dispersed within the polymer matrix. These nanoparticles typically lie in the nanometer range and act as reinforcement to achieve functional properties. These materials have attracted the research focus due to their extraordinary enhancement in mechanical, thermal, electrical, or chemical properties even at very low reinforcement content [45,46]. Polymer nanocomposites provide an added benefit of homogeneity than fiber-reinforced composites, as they are less prone to anisotropic effects induced due to unidirectional reinforcement. Various nanoparticle-based composites have been developed for AM processes and mainly

focused on improved mechanical and electrical properties. For example, nanoclay for improved mechanical [47–49], carbon nanotubes, and graphene for improved electrical conductivity [50–53] are reported in the literature.

This section provides an overview of recent progress in nanocomposites for AM processes for improved mechanical, thermal, or electrical properties. Table 2 presents the highlights of different polymer nanocomposites fabrication via AM processes and their improved properties.

#### 3.1. Polylactic acid (PLA) – based polymer nanocomposites

Polylactic acid (PLA) is a thermoplastic polyester, generally obtained from biodegradable resources, and exhibits excellent mechanical and thermal properties, good processability, and low impact on the environment [54]. PLA is globally accepted as biodegradable due to its origin from plants and has proven safe for biomedical applications and food industries [55]. Therefore, being explored in tissue engineering, biomedical implants, and food packaging sectors for their performance and processing through AM processes [56]. PLA is commercially available and can be purchased from Ultimaker, Stratasys, and 3dxtech companies.

In addition to the sustainability aspect, it needs to be strengthened mechanically for improved performance. Hydroxyapatite (HA) has proven an effective reinforcement to PLA for mechanical strength and biocompatibility. Petrovskaya et al. [57] synthesized PLA-based composite

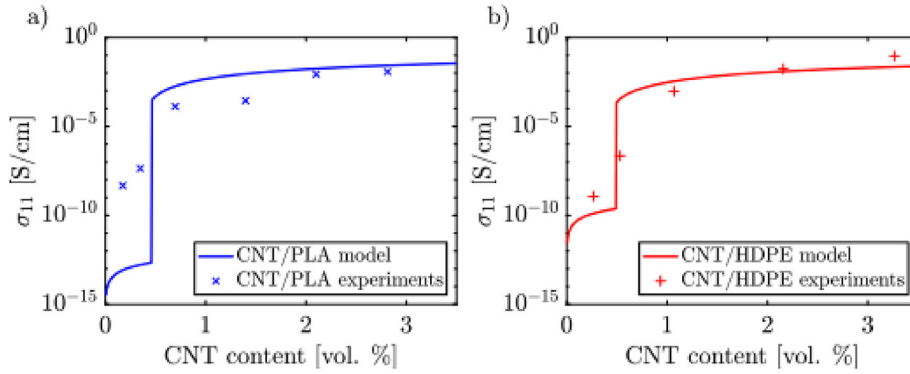


**Fig. 6 – Comparison of Theoretical model and Experimental Results for Electrical conductivity (a) PLA/CNT and (b) HDPE/CNT nanocomposites (Reproduced with Permission from [62]).**

materials with varying HA contents (0–30%). The composites obtained were granulated, processed into filaments using a screw extruder, and 3D printed via a commercial FFF 3D printer. Extrusion temperature, printing temperature, and printing speed were optimized for all the mix proportions. Compression, flexural and impact tests were also performed on samples for mechanical characterization. Among all the materials tested, composites with 30% HA contents exhibited maximum compression, flexural, impact strengths and withstood the maximum number of loading cycles, which was higher than the individual strengths of constituents. In another study, Wu et al. [58] attempted to explore applying the FFF process in the 3D printing of bone implants. 5, 10, and 15% HA reinforced PLA polymer composites were prepared through the solution mixing process, subsequently molded to filament using a single screw extruder. Compositional, microstructural, and mechanical characterization was performed on 3D printed scaled-up trabecular bone models and standardized compression test samples. Microstructural analysis revealed that basic trabecular bone structure could be reproduced via 3D printing. The incorporation of HA in the PLA matrix improved mechanical properties for bulk and 3D printed trabecular bone models at different scales (as presented in Fig. 5) but reduced the print quality was observed. Backes et al. [59] reported improved composites thermo-mechanical properties. Increased cell proliferation was observed at 10% HA content. PLA/HA nanocomposites were synthesized through melt processing techniques following

the microstructural, mechanical, and thermal analysis. FFF filaments were also prepared, and the process demonstrated the feasibility of PLA/HA nanocomposites for AM applications. 3D printed nanocomposites unveiled appropriate print quality and accuracy.

Coppola et al. [60] investigated Cloisite (nanoclay) reinforced PLA nanocomposite filaments for the FFF process. 4 wt% of nanoclay was added to PLA. PLA/nanoclay composites revealed better shape stability with an improved degree of crystallinity, storage modulus, tensile modulus, and thermal stability. Carbon-based reinforcement, i.e., carbon nanotubes (CNTs), carbon nanofibers (CNFs), graphene, and carbon black, is also reported to enhance the mechanical and electrical properties of PLA-based 3D printed parts. Beniak et al. [61] performed the mechanical and electrical characterization of 3D printed carbon black reinforced PLA nanocomposites. A strong impact of infill volume and infill type on the composites' mechanical properties was noticed. Better strength was observed for rectilinear infill with 90% infill volume, and in addition to that, higher nozzle temperatures also resulted in lower electrical resistivity. Likewise, Mora et al. [62] used the melt blending technique to fabricate FFF filaments for PLA/CNT and HDPE/CNT nanocomposites. Different reinforcement contents were introduced to the base material, and electrical conductivity was measured for each material. The micromechanics-based model was developed to predict the electrical conductivity in the case of segregation of CNTs.

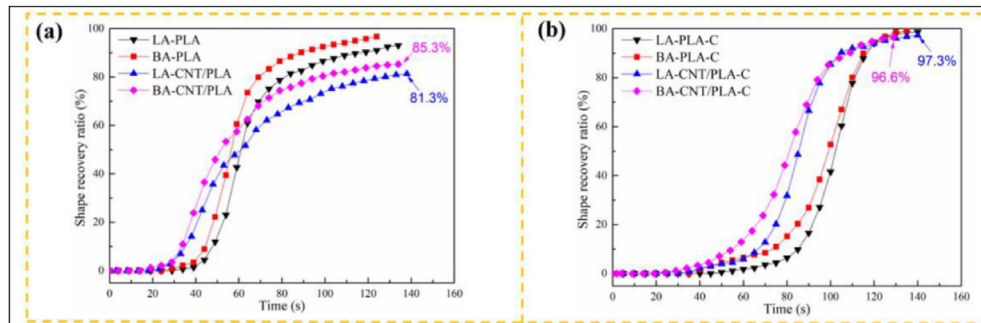


**Fig. 7 – Characterization of shape recovery ratio (a) 4D printed PLA and CNT/PLA ± 45° angle-ply laminated preform (LA) and rectangular braided (BA) preforms and (b) their silicone matrix composites (Reproduced with Permission from [63]).**

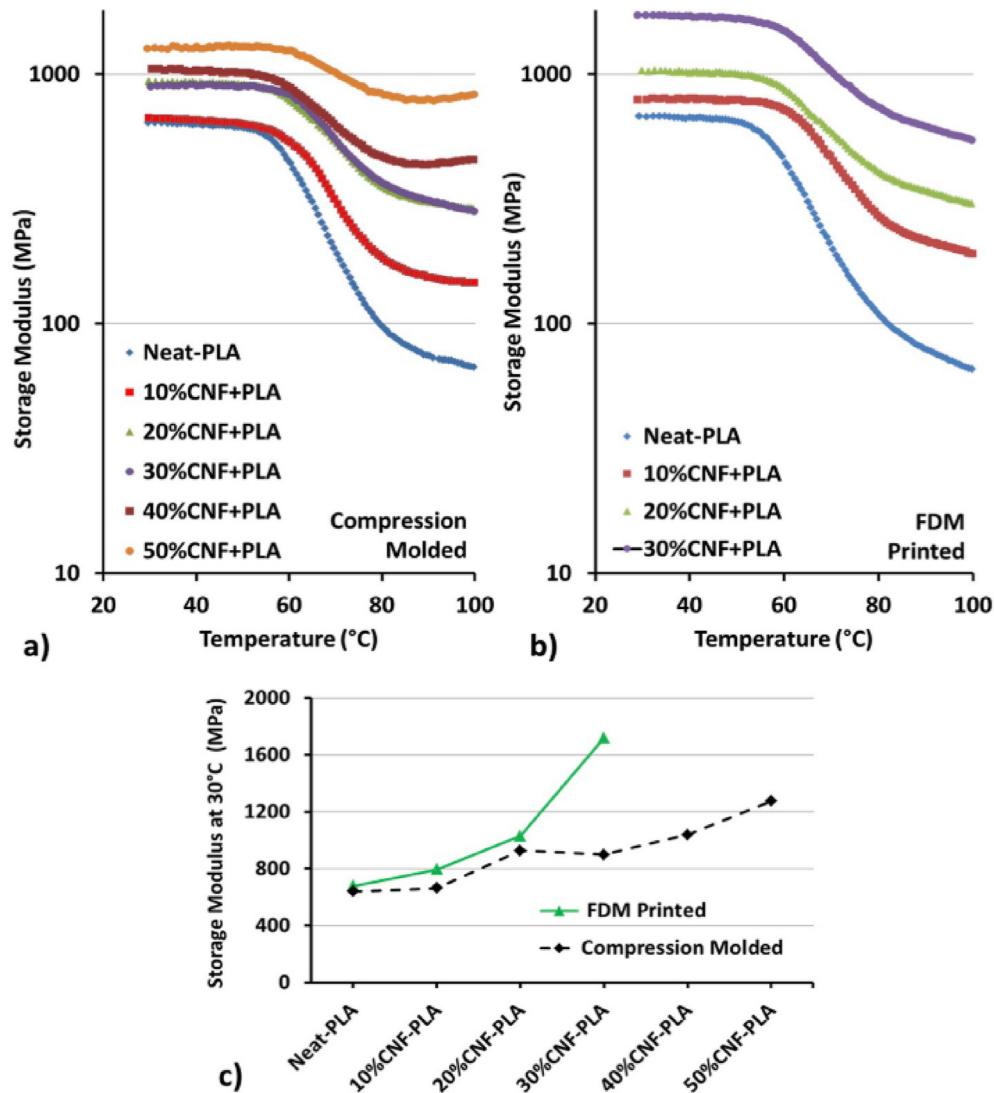


**Fig. 8 – Dynamic Mechanical Properties of PLA/cellulose nanofiber composites. (a) Storage modulus of compression-molded PLA and composites (b) Storage modulus of 3D Printed PLA and composites (c) Comparison of Peak Value (Reproduced with Permission from [64]).**

The theoretical model results agreed well with the experimental outcomes (as reported in Fig. 6). Therefore, the model can design polymeric nanocomposites with agglomerated particles.

CNTs have also evidenced effective reinforcement for shape memory polymers, as Liu et al. [63] reported, in which CNT-reinforced PLA nanocomposites for shape memory applications were fabricated. Microstructural, shape memory behavior, and mechanical testing were performed on 4D printed nanocomposites. Results revealed improved recovery force (up to 144%) and flexural strength of the material with the inclusion of CNTs. A shape memory ratio of 97.3% was also observed due to the inclusion of the silicone matrix (Fig. 7).

Cellulose nanofibers reinforced composites have provided remarkable results in synthesizing and fabricating sustainable materials with significant mechanical properties. Tekinalp et al. [64] fabricated cellulose nanofibers reinforced PLA-based composites following microstructural, thermal,

mechanical, and dynamic characterization. Considerable improvement in tensile strength and elastic modulus was observed. Synthesized material was also fed to the FFF machine, and 3D printed samples were tested for their mechanical properties. 3D printed specimens also revealed improved elastic strength and storage modulus (Fig. 8). Zhang et al. [65] utilized reduced graphene oxide (rGO) as filler material to PLA for flexible circuits. PLA/rGO nanocomposites were synthesized through the melt compounding process. A significant improvement in electrical conductivity was observed for a 4 to 6 wt% increase in rGO concentration. It was also concluded that the percolation threshold for rGO lies in between 4 and 8 wt%. The authors believed that improved electrical conductivity was achieved due to nanoparticle alignment owing to the extrusion process.

The PBF process utilization has also been reported in the literature to 3D print PLA polymer nanocomposites. Gayer et al. [66] attempted solvent-free material processing for the

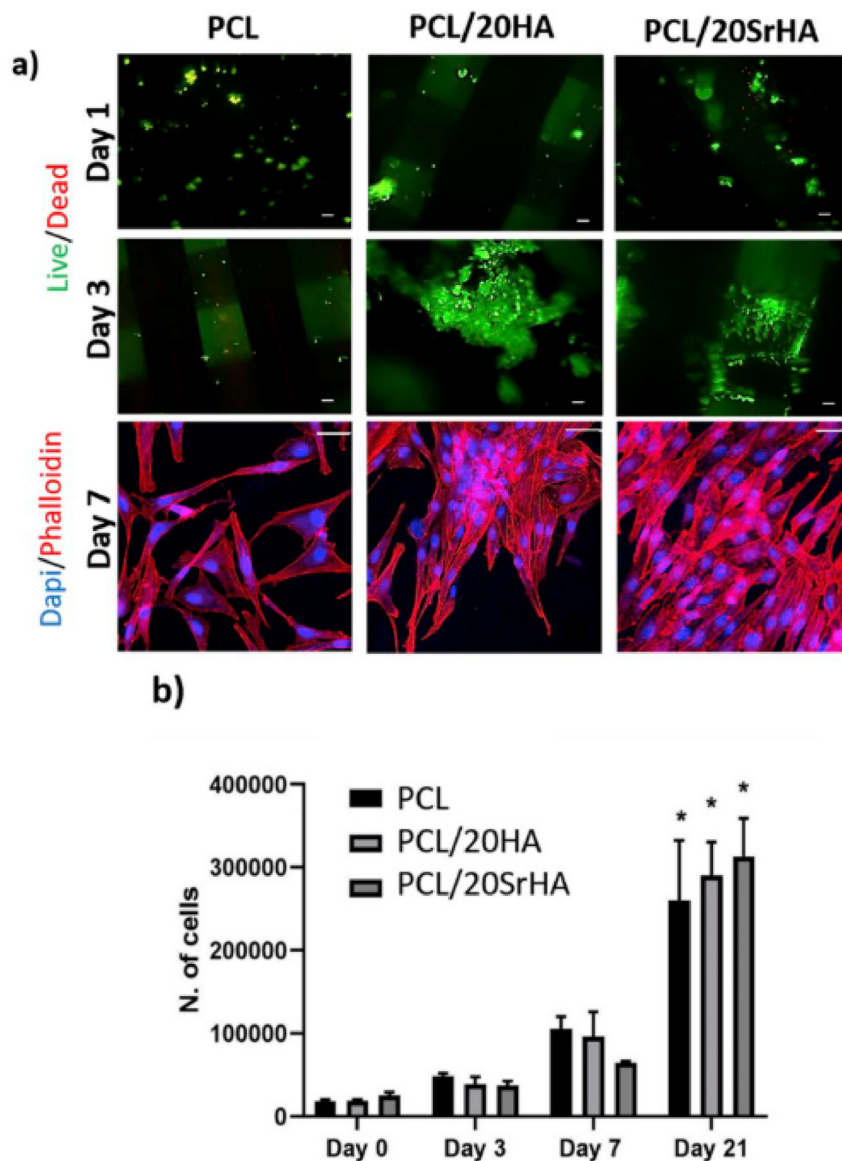


**Fig. 9 – (a) Cytocompatibility of PCL and PCL/SrHA Nanocomposites (Day 1- 7) (b) Estimation of number of cells using MTT absorbance up to 21 Days (Reproduced with Permission from [68]).**

selective laser sintering (SLS) process. PLA/calcium carbonate (CC) composites powder was developed, containing 75% and 25% of PLA and CC. Different PLA grades were analyzed, and nanocomposites with the lowest inherent viscosity were observed to have the SLS process's best processability. Careful selection of process parameters enabled researchers to produce 3D-printed parts without loss in inherent viscosity. The manufactured parts revealed maximum biaxial bending strength of 75 MPa and micro-porosity around 2% only.

### 3.2. Polycaprolactone (PCL) – based polymer nanocomposites

PCL is also an approved biodegradable material by the US Food and Drug Administration (FDA); therefore, its applications in biomedical engineering have been explored [67]. Some processes

are also reported in the literature to 3D print this material owing to its suitability in bone tissue engineering. Pierantozzi et al. [49] introduced a novel extrusion-based process for 3D printing composite scaffolds to explore PCL utilization in biomedical applications. PCL matrix containing the bioactive reinforcing phase of HA and strontium substituted HA (SrHA) were printed directly, eliminating the need to produce filaments, thus avoiding a multi-step manufacturing process. The resulting composites with varying reinforcing content were characterized for their physical, mechanical, and biological properties. Different architectures were designed to mimic the bone tissue structure, and printing parameters were optimized for different material configurations. Micro-CT analysis revealed that the porosities of 3D printed samples were in good agreement with 3D CAD models, proving the reliability of the introduced process. No correlation was found between the mechanical properties of

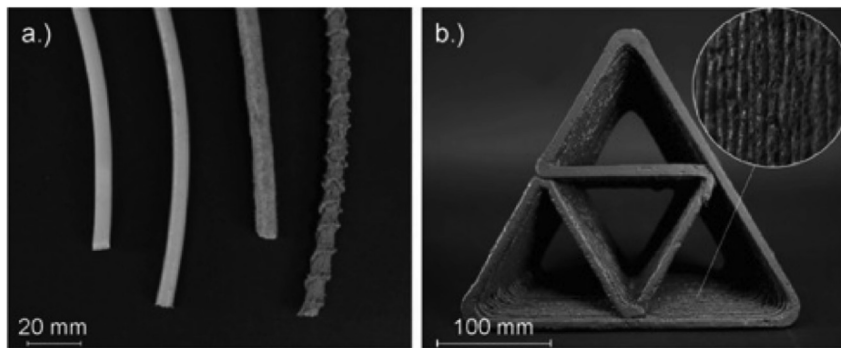


**Fig. 10 – (a) HDPE, HDPE/Cardboard-20%, HDPE/Cardboard-50%, HDPE/Cardboard-75 (Left to Right) (b) 3D printed object fabricated using HDPE/Cardboard-50% filament (Reproduced with Permission from [70]).**

nanocomposites and their formulations. However, filler addition revealed biocompatibility of the material and improved mineralization for PCL/SrHA composites, as shown in Fig. 9.

### 3.3. High-density polyethylene (HDPE) – based polymer nanocomposites

HDPE is the most widely used polymer in the consumer industry. It exhibits a high strength-to-density ratio as compared to LDPE. However, HDPE's two most essential concerns include; its reusability and lower mechanical strength [69]. HDPE-based composite filaments incorporated with cardboard dust particles were prepared for the FFF process to overcome the problem of recycling [70]. Different cardboard dust contents (20, 50, and 75%) were added to HDPE, and resulting nanocomposite filaments were analyzed for their microstructural and mechanical properties. The filament was extruded successfully without considerable deviation in diameter and density for lower cardboard content; however, loss in density and larger filament diameter was observed for higher filler contents. Degradation of mechanical properties and glass transition temperature was also observed for an increased ratio of cardboard dust particles; however, the 3DP process was still applicable at these percentages. Fig. 10 presents the successfully 3D printed object fabricated using 50% cardboard content in HDPE.

CNTs could also provide significant improvements in HDPE composites. Mora et al. [62] used the melt blending technique to fabricate FFF filaments for HDPE/CNT composites. Different reinforcement contents were introduced to the base material (HDPE), and electrical conductivity was measured for each material. The resulting composites were evaluated to be suitable for electro-conductive applications.

### 3.4. Acrylonitrile butadiene styrene (ABS) – based polymer nanocomposites

ABS is an exciting material for the fabrication of polymer composites; due to its solubility in acetone, which assists the synthesis of composites, it can hold higher filler content and is easily extrudable [71]. ABS is commercially available under different brand names and can be purchased from Ultimaker, Stratasys, MakerBot, and 3dxtech. It has the advantages of

good flexural and impact strength, resistance against the chemical environment, and good physical stability [72,73]. However, to improve its thermal and electrical performance, the addition of metallic particles to ABS evidences its utilization in electrical and thermal conductivity applications. Palermo et al. [71] performed a microstructural and morphological evaluation of ABS polymer composites reinforced with metallic particles (aluminum and stainless steel). Optimum values of metallic reinforcement were obtained for both reinforcing materials, following the successful extrusion of the composite filament by the FFF process. The effect of particle size and distribution on the physical properties of composites and FFF filaments was demonstrated. Results provided an adequate basis route for the development and deployment of novel materials to 3DP processes. It was concluded that with achieved high filling ratios, tailored materials with the desired number of metallic particles could be introduced to achieve desired thermal and electrical properties.

Similarly, Hamzah et al. [74] performed the mechanical, electrical, and thermal analysis of 3D printed ABS/ZnFe<sub>2</sub>O<sub>4</sub> composites. The effect of reinforcement particle contents and raster angle was studied on the examined properties of the composites. Raster angle did not affect the properties much; however, improved tensile strength, hardness, thermal conductivity, and electrical conductivity were observed for high filler ratios.

Several studies report the utilization of clay-based nanoparticles as reinforcement to polymers. Weng et al. [48] investigated the mechanical and thermal properties of ABS reinforced with montmorillonite nanoparticles for the FFF process. Montmorillonite clay was modified using benzyl-dimethyl hexadecyl ammonium chloride (HDBAC) for variable loadings (1, 3, and 5 wt%). ABS polymer was melt compounded with nanoclay using a twin-screw extruder. Higher void content and lower polymer chain entanglement were observed for FFF parts than injection molded parts, resulting in inferior mechanical properties. Improved mechanical properties were achieved for higher reinforcement contents (Fig. 11). At higher nanoclay concentration (i.e., 5 wt%), mechanical properties did not reveal a significant effect of the fabrication method.

Francis et al. [49] developed ABS/OMMT nanocomposites through solution mixing technique for ABS filament coating and their application in microwave and radio components.

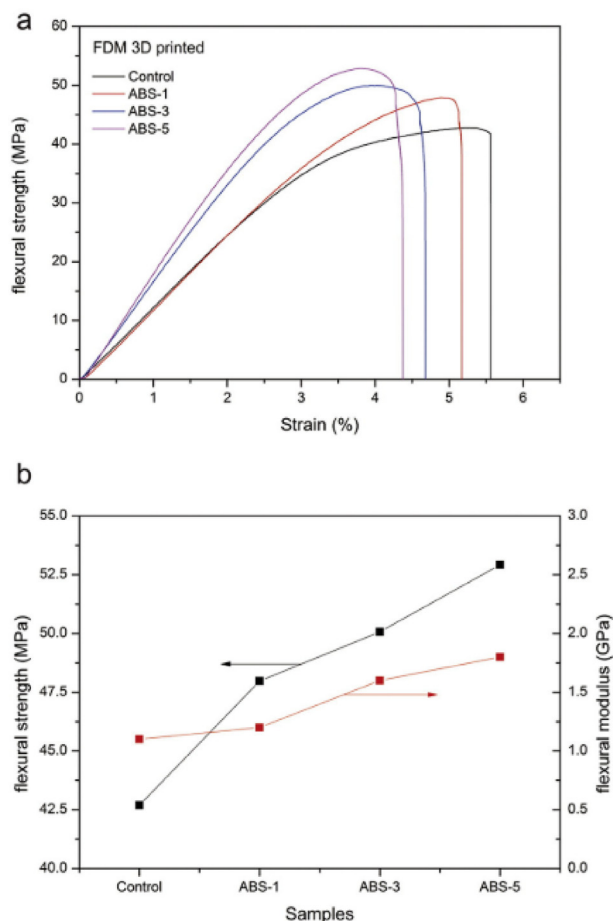


**Fig. 11 – (a) Flexural Stress vs. Strain strength (b) Flexural strength & Flexural Modulus of 3D Printed ABS/OMMT nanocomposites (Reproduced with Permission from [48]).**

The OMMT concentration was 3 wt%. ABS core and ABS/OMMT shell nanocomposite filament were placed in microwave for better interfacial adhesion of two phases. 3D printed components revealed an improved tensile strength and hardness. Meng et al. [47] analyzed four different nanoparticle reinforcements (montmorillonite (MMT), multi-walled carbon nanotubes (MWCNT), calcium carbonate ( $\text{CaCO}_3$ ), and silica ( $\text{SiO}_2$ )) to ABS at a fixed concentration of 1 wt% using a twin-screw extruder. MMT nanocomposites revealed the highest tensile and flexural strength; however,  $\text{CaCO}_3$  reinforcement significantly improved the failure strain. Besides, the effect of printing orientation was also analyzed, where horizontally printed specimens provided better mechanical properties.  $\text{CaCO}_3$  reinforcement to ABS also resulted in reduced material anisotropic behavior.

Carbon-based nanoparticle reinforcements have attracted researchers to fabricate functional nanocomposites through AM processes for electrical and electronics applications [52,65,75]. Dorigato et al. [76] introduced varying concentrations (1–15 wt%) of MWCNTs to ABS polymer using a twin-screw extruder and produced nanocomposite filaments for the FFF process. The addition of MWCNTs drastically improved the electrical conductivity and

mechanical properties; however, at the cost of reduced failure strain. 3D printed nanocomposites also revealed lower specific heat and improved thermal conductivity. Similarly, Dul et al. [77] fabricated ABS/MWCNT nanocomposites with variable loadings (0–8 wt%) through the melt blending technique. Comparable mechanical and electrical properties were observed, as reported by Dorigato et al. [76]. Optimum properties were achieved at a 6 wt% concentration of MWCNTs.

Graphene nanoparticles are widely reported to improve the thermal and mechanical properties of thermoplastics [53]. For the first time, Wei et al. [84] utilized reduced graphene oxide (rGO) as a reinforcing phase to ABS via solution mixing for the FFF process. GO, owing to the presence of functional groups, provided better dispersion than pristine graphene. Results revealed a dramatic increase in electrical conductivity due to the presence of rGO. Similarly, Dul et al. [53] synthesized graphene reinforced ABS nanocomposites through melt blending for the FFF process. Different graphene concentrations (2, 4, and 8 wt%) were analyzed for tensile and melt flow behavior to achieve the optimum properties. Elastic modulus was observed to increase with increasing graphene concentration; however, melt flow index and tensile strength decreased due to poor adhesion between graphene and ABS (Fig. 12). Dul et al. concluded 4 wt% content of graphene as optimum in terms of MFI and mechanical properties.

Yamamoto et al. [78] developed GO reinforced ABS nanocomposites through solution mixing technique for the FFF process. Varying GO concentrations (0.02, 0.04, and 0.06 wt%) were analyzed for mechanical properties. Reduced failure strain and toughness were observed; however, increasing GO concentration tensile strength and stiffness were improved. The maximum improvement in mechanical properties was noticed at 0.06 wt% GO content (i.e., 29% and 55% increase failure strain and toughness, respectively).

### 3.5. Polyvinylidene fluoride (PVDF) – based polymer nanocomposites

Typically, the extrusion process for PVDF is challenging due to the high coefficient of thermal expansion. The inclusion of materials with a low thermal coefficient could make it feasible for AM by tailoring the composite material properties. To study the impact of metallic particles with a negative coefficient of thermal expansion, Momenzadeh et al. [79] synthesized zirconium tungstate (1–10%) reinforced PVDF composites for the FFF process. Zirconium tungstate facilitated the provision of improved printability of the composites by lowering the overall thermal expansion. Although improved dimensional accuracy was achieved using reinforcing components, it was attained at the expense of reduced mechanical strength and elongation compared to pure PVDF. Kim et al. [80] investigated the piezoelectrical response of PVDF with the introduction of MWCNT and barium titanate (BT) nanoparticles for the FFF process. MWCNTs assisted the higher concentration of  $\beta$ -phase with polymers which resulted in improved piezoelectrical efficiency. The highest piezoelectric coefficient (i.e., 129 pC/N) was achieved for 0.4 wt% of MWCNTs and 18 wt% of BT concentration. Using TPU/MWCNT

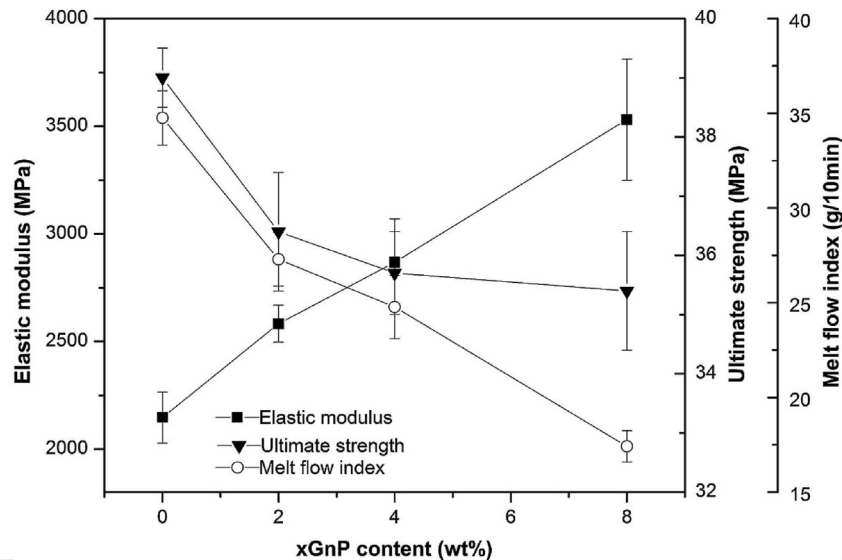


Fig. 12 – Elastic Modulus, Ultimate Strength and Melt Flow Index of ABS & ABS/Graphene Nanocomposites (Reproduced with Permission from [53]).

nanocomposites, the authors were able to 3D print multiaxial force sensors. In addition, structural and sensor components were simultaneously 3D printed using a dual-extrusion head, simplifying the sensor fabrication process.

### 3.6. Thermoplastic polyurethane (TPU) – based polymer nanocomposites

TPU is a biocompatible material with excellent mechanical properties and is widely used as a coating material to biomedical implants [81]; however, it can be further enhanced with nanoparticle reinforcement for functional applications. TPU is commercially available from Ultimaker and Stratasys companies. Christ et al. [51] synthesized MWCNTs reinforced (1–5 wt% concentrations) TPU nanocomposites for sensors

applications. The authors noticed a linear increase in elastic properties with increasing MWCNT concentrations. A good interlayer adhesion between printed layers was observed, which resulted in improved electrical conductivity (Fig. 13). It was concluded that the piezo sensitivity of the TPU/MWCNT nanocomposites could be tuned with varying reinforcement content. Likewise, Hohimer et al. [82] investigated the mechanical properties and effect of printing orientation for similar nanocomposites using the FFF process at 1 and 2 wt% reinforcement of MWCNTs. The introduction of nanoparticles improved the elastic modulus; however, elastic strength and failure strain decreased. Better mechanical properties were observed for axially printed specimens due to better interfacial adhesion than specimens printed in the transverse direction.

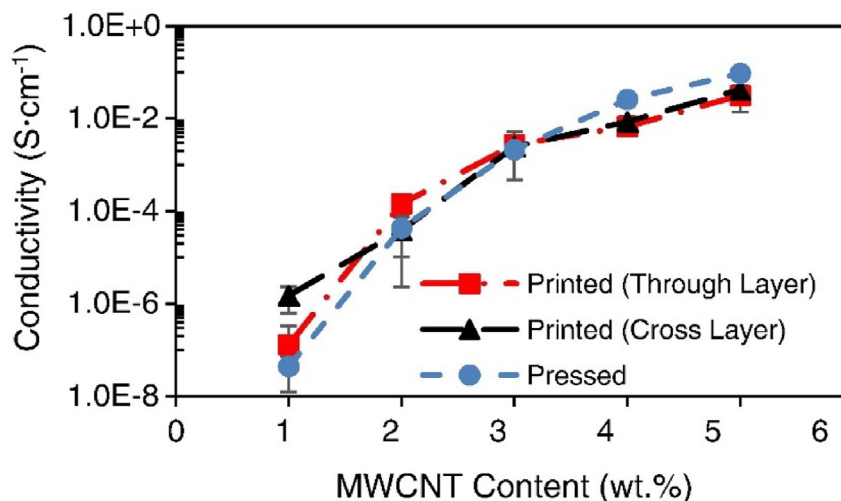
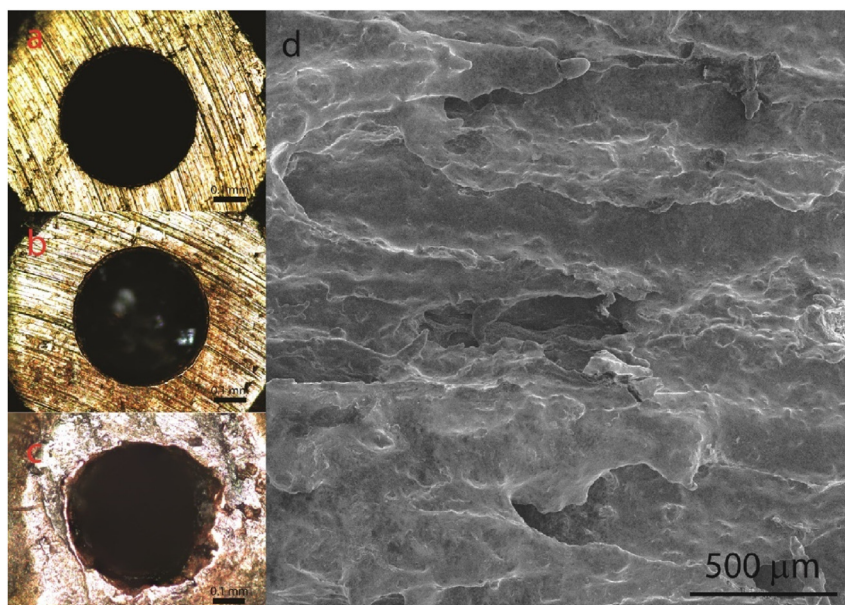


Fig. 13 – Electrical conductivity vs. MWCNT content for pressed and 3D Printed TPU/MWCNT nanocomposites (Reproduced with Permission from [51]).



**Fig. 14 – Optical Images of (a) Unused Nozzle (b) Nozzle after printing 10 cm PBT/Graphene (c) Nozzle after printing 1.5m PBT/CNT (d) SEM image of PBT/Graphene composite printed with an abraded nozzle (Reproduced with Permission from [83]).**

### 3.7. Polybutylene terephthalate (PBT) – based polymer nanocomposites

Gannasekaran et al. [83] synthesized carbon nanotubes and graphene reinforced PBT nanocomposites via solution mixing process for the FFF process. Graphene/PBT revealed a rough surface and brittle behavior than CNT/PBT filaments. The electrical conductivity percolation threshold PBT nanocomposites were calculated as 0.49 wt% of CNT and 5.2 wt% of graphene, respectively. The calculated values agreed well with the experimental results. Significant nozzle wear was also observed due to the presence of abrasive carbon nanoparticles (Fig. 14).

### 3.8. Nylon–based polymer nanocomposites

Polyamide (also referred to as Nylon) is utilized due to its significant mechanical properties. Nylon reinforcement with nanoparticles can provide heat and chemical resistance. Nylon 6 is commercially available from Stratasys and 3Dxtech. However, Nylon 12, also known as polyamide 12 (PA12) and fiber-reinforced Nylon grades, can be purchased from Stratasys. PA12 exhibits a semi-crystalline structure and is the most widely used material in PBF processes due to its higher melting point and glass transition temperature [84]. PA12 can provide high impact strength but prone to be affected by moisture [85]. Zhu et al. [86] evaluated thermal and mechanical properties of graphene varying (1–10 wt%) reinforced polyamide 12 (PA12) nanocomposites. The synthesized nanocomposites revealed lower crystallinity and better thermal resistance, and the graphene agglomeration was prominent. 6 wt% of graphene content was found optimum for tensile, thermal, and FFF processing.

The serviceability of PBF for 3DP of PA12 composites was performed by Connor and Dowling [87]. They investigated the

physical, chemical, and mechanical properties of pure PA12 and PA12 reinforced with glass spheres (40% by volume). A production-scale AM process, known as the multi-jet fusion (MJF) process, was used to 3D print the specimens in different orientations, as presented in Fig. 15. It was observed from thermal and chemical analysis that both materials exhibited the same properties. Results revealed an improved tensile and flexural modulus but lower strength and elongation when compared with pure polymer (Fig. 16). Build orientation strongly affected the strength and porosity of 3D printed specimens (Fig. 17). SEM analysis of fractured surfaces discovered poor interfacial bonding between the two phases; however, homogenous structure and porosity (<1%) were observed for pure polymer and composite.

Chunze et al. [88] used nanosilica to reinforce PA12 powder for improved thermal and mechanical properties. The results revealed a 20.9% increase in tensile strength, 39.4% in elastic

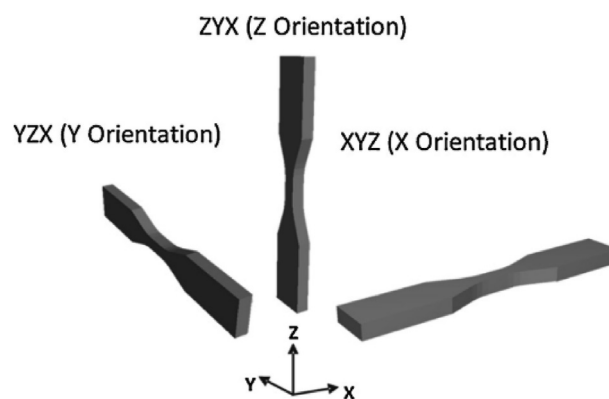


**Fig. 15 – Schematic of ASTM Standardized Specimens 3D Printed in different orientations (Reproduced with Permission from [87]).**



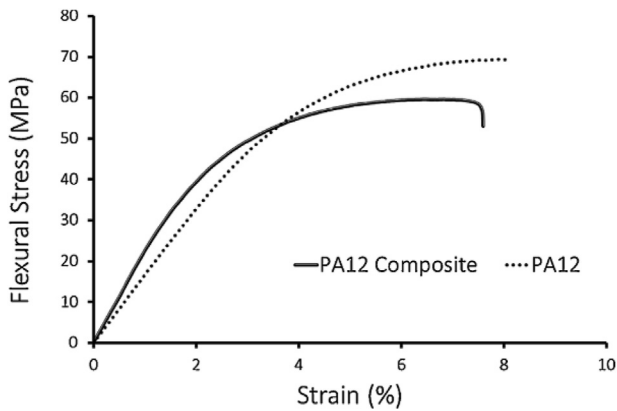


**Fig. 16 – Flexural Stress vs. Strain of PA12 and PA12 Composites (3D Printed in Z-Direction) (Reproduced with Permission from [87]).**

modulus, and 9.54% in impact strength; however, failure strain was decreased by 3.65%.

Athreya et al. [89] developed carbon black reinforced Nylon 12 nanocomposites for the SLS process with improved electrical conductivity. The experimental results revealed reduced flexural modulus owing to weak interfacial bonding between PA12 and carbon black. However, a dramatic increase in electrical conductivity (5 times) was observed with a low percolation threshold (Fig. 18). In another study, MWCNTs were introduced to PA12 for the SLS process. PA12/MWCNTs nanocomposites revealed a 10% increase in tensile strength; however, elongation to break was reduced by 11% [90]. In addition, a significant improvement in fatigue strength was observed for 0.5% MWCNTs content to PA12 (Fig. 19).

Goodridge et al. [91] investigated the use of carbon nanofillers to PA12 for the SLS process. Results revealed an increased storage modulus for PA12/carbon nanofillers composites up to 22%. The suitable powder size and morphology were pointed out as a significant challenge for the SLS process. Koo et al. [92], Cheng et al. [93], and Moore et al. [94] performed extensive experimental studies on PA11 and PA12 materials with MMT, CNFs, and MWCNTs as reinforcement phases. Enhanced thermal & mechanical properties, as well as flame

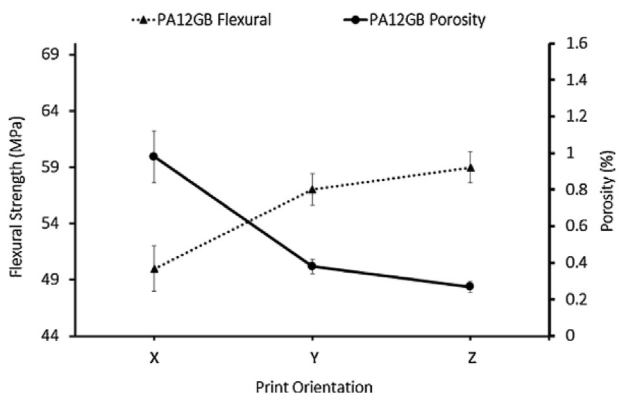


**Fig. 17 – Flexural Strength and Porosity (%) of PA12/Glass bead Composites at different printing orientations (Reproduced with Permission from [87]).**

retardancy, were achieved. The authors were able to 3D print high-density and complex structures using PA11/CNF nanocomposites. Nanoclay and CNFs incorporation to polymers provided reduced flammability properties.

Metal-based nanoparticles have also proved their potential as reinforcement to polymers, as they can provide improved material solidification and mechanical properties. Polyamide reinforced with nano aluminium oxide particles revealed improved tensile strength with increasing particle concentration [95]. In another study, aluminium oxide nanoparticles coated with polystyrene provided increased tensile strength (up to 300%) and notched impact strength (up to 50%) for the SLS process [96].

### 3.9. Photopolymers & epoxies – based polymer nanocomposites

Photopolymers are light-sensitive materials, normally polymer monomers, which solidify on exposure to radiation [97]. The range of wavelength, which causes these materials to cure depends upon their nature. Therefore, a variety of light sources could apply to the vat polymerization technique. In addition to the development of processes, biodegradable materials have attracted researchers owing to their sustainability. One of these green materials is cellulose, which has proven to be a significant reinforcement to polymer-based materials. Still, such material's utilization is limited due to dispersion issues [98]. Mohan et al. [98] attempted to produce cellulose nanofibers reinforced PU-based photopolymer composites. Cellulose nanofibers were treated with polyethylene glycol (PEG) and rGO to improve their compatibility with epoxy. The vat photopolymerization process was utilized to cure photo-sensitive PU epoxy. The resulting nanocomposites were analyzed for the dispersibility of cellulose nanofibers in epoxy, chemical, and mechanical properties. Results revealed maximum tensile strength and hardness for a 3% addition of cellulose nanofibers. Fig. 20 presents the stress–strain curves for cellulose nanofibers treated with PEG and rGO. Furthermore, the best dispersion of nanoparticles within the material was observed for the same ratio of reinforcement.

Clay reinforced photopolymer resins provide improved mechanical properties and resin reactivity. Corcione et al. [99] investigated the compatibility and resin reactivity for organically modified MMT clay (Dellite 43B) with photo resin (UV 6105). The nano resin reactivity improved by 15% with 0.3 wt% nanoclay; however, it decreased with further addition. It was concluded that nanoclay particles act as diffusion aiding agents at lower loadings and assist the photopolymerization reaction, resulting in improved curing; however, at higher concentrations (i.e., 1.0 wt%), these particles hinder the photopolymerization reaction. The agglomeration of nanoclay particles could also be the reason for declined curing rate of the resin. Weng et al. [100] also studied MMT and attapulgite nanoclay reinforced photopolymer resins. An improved elastic modulus was observed for both types of nanoparticles. MMT revealed enhanced tensile strength at lower loadings.

Polymers with suspended magnetic particles have found their electrical and electronic devices applications as they become responsive to the magnetic field. Nagarajan et al. [101]

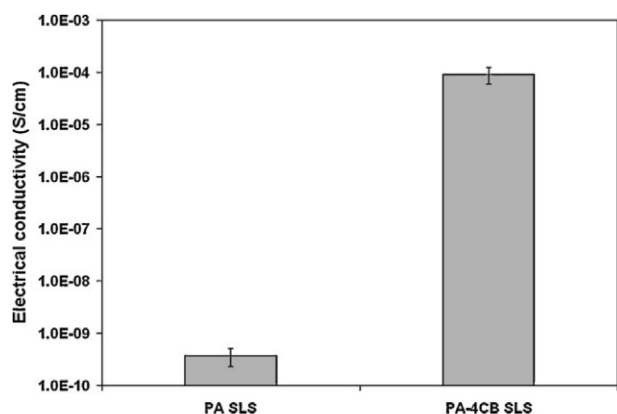


**Fig. 18 – Electrical conductivity of PA and PA/4%-Carbon Black Composites 3D Printed via SLS (Reproduced with Permission from [89]).**

used the stereolithography technique to 3D print magnetic particles suspended in the polymer. UV curable prepolymers were mixed with 5% magnetic particles ( $\text{SrFe}_{12}\text{O}_{19}$ ) and varying content of rheological additive (0.2%–0.6%). The stability of suspended particles within any mixture is vital for the homogenous dispersion of these particles within the composites; therefore, it was analyzed. Fig. 21 shows nanoparticle suspensions using different rheological additive contents in prepolymer immediately after mixing and after 1.5 h. 0.4% additive content was found appropriate to provide stable suspension and was selected for 3D printing samples. 3D printed samples were analyzed using scanning electron microscopy (SEM), coordinate measuring machine (CMM), and Fourier transform infrared spectroscopy (FTIR). Aggregation of magnetic particles between printed layers was observed in the microstructural and dimensional analysis of printed samples due to attraction between these particles. The dimensional inconsistencies were also observed and were attributed to selected printing parameters.

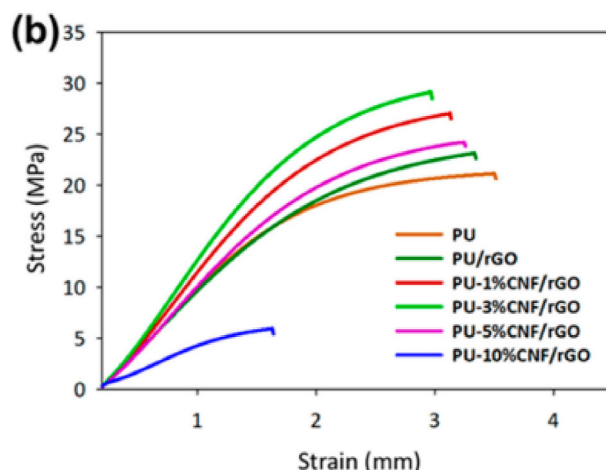
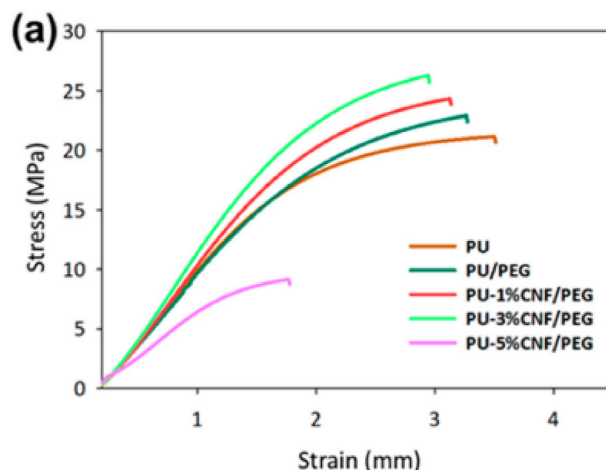


**Fig. 20 – Stress vs. Strain Diagrams for 3D Printed PU-Resin reinforced with cellulose nanofibers treated with (a) PEG and (b) rGO (Reproduced with Permission from [98]).**

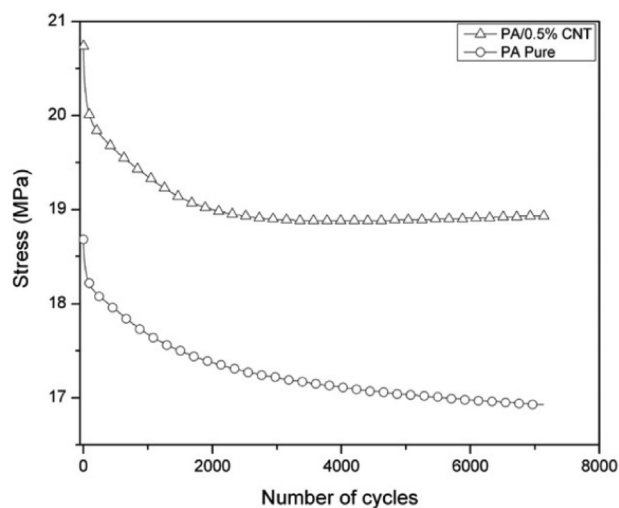


**Fig. 19 – Fatigue strength as a function of cycle number for PA and PA/MWCNTs composite (Reproduced with Permission from [90]).**

Higher filler percentages are desired for improved thermal or electrical conductivity of composites. Nevertheless, the higher content of filler within the polymer matrix hinders the utilization of AM processes. Lu et al. [102] presented a novel technique for 3D printing of polymer composites with patterned fillers (aluminum powder) within the matrix, termed acoustic field-assisted projection stereolithography (A-PSL). A schematic diagram of the process used is presented in Fig. 22. Piezo elements were utilized to formulate filler structures within the polymer suspension. Subsequently, the suspension was cured to produce polymer composites with structured fillers. 3D printed components revealed enhanced heat dissipation capabilities for the same amount of filler content within the polymer matrix as in uniform composite.

Likewise, Malas et al. [103] developed a novel material for the vat photopolymerization process and investigated its different physical and electrical properties. Composite resin was produced by adding titanium dioxide (nano-mesh) or calcium copper titanate (micro-mesh) in a photopolymer. Structural, thermal dynamic, and dielectric properties were

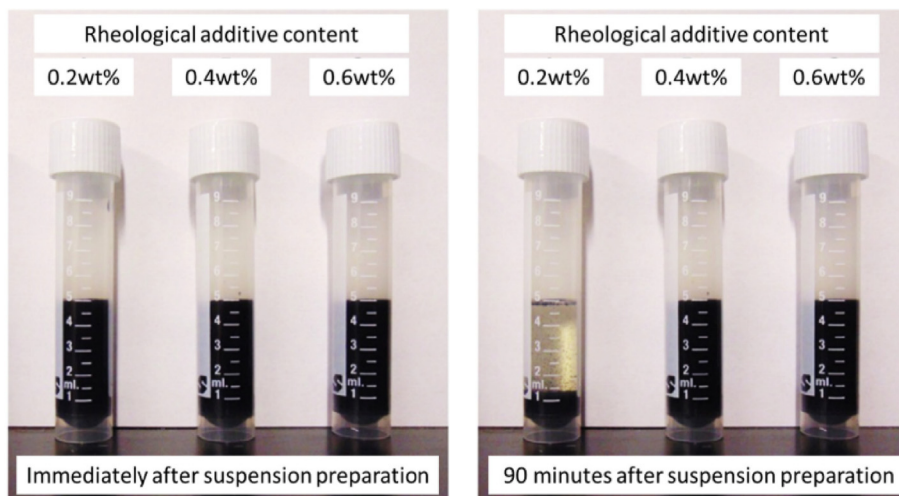


**Fig. 21 – Nanoparticle suspensions using different rheological additive contents in prepolymer immediately after mixing and after 1.5 h (Reproduced with Permission from [101]).**

accounted for to evaluate the material performance. Different reinforcement percentages were employed to observe the effect of additives on composite viscosity. Titanium dioxide polymer composite revealed comparable surface morphology compared to neat polymer. However, fractured samples exhibited rough surfaces contrary to control filler-free polymer resin's smooth surfaces. At 20% content by weight of reinforcing particles, increased glass transition temperature, storage modulus, and dielectric permittivity were also observed (Fig. 23).

In addition to higher filler content, faster curing helps maintain homogeneity and desired properties of 3D printed

parts. Choong et al. [104] fabricated photopolymers reinforced with nano-silica through the digital light processing (DLP) technique. Nano-silica particles served as catalysts and reduced the curing time of photopolymers. Fig. 24 presents the schematic diagram of phenomena involved in polymerization assistance due to nano-silica particles. Mechanical, optical, and thermal characterizations were performed on additively manufactured shape memory polymers (SMP). Results revealed an improved mechanical strength of composites and also remarkable shape memory characteristics. A recent study reported a novel photo-cross-linkable nano-composite synthesis composed of methacrylate polymer and

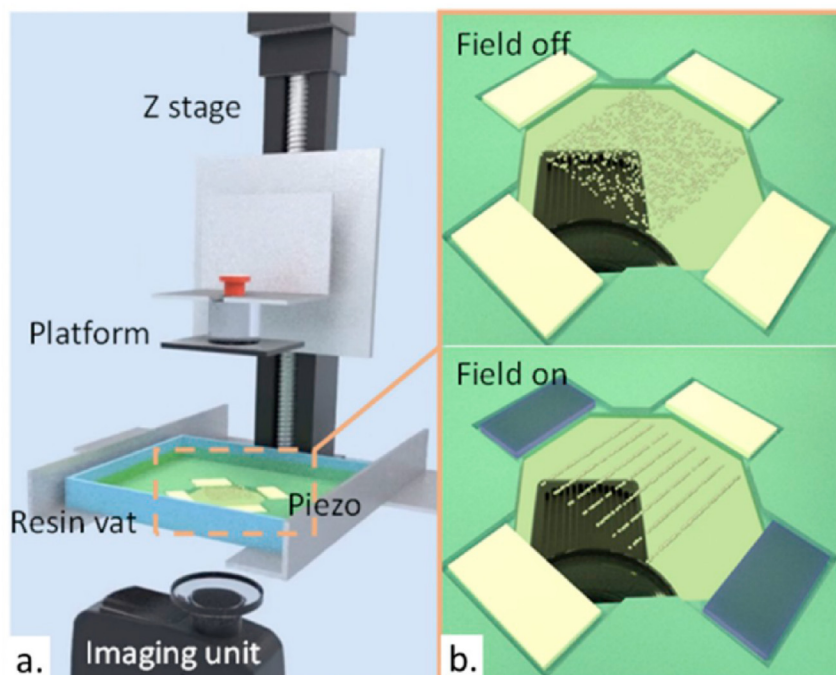


**Fig. 22 – Schematic diagram of (a) acoustic field-assisted projection stereolithography (A-PSL) (b) Acoustic field-assisted filler assembly (Reproduced with Permission from [102]).**

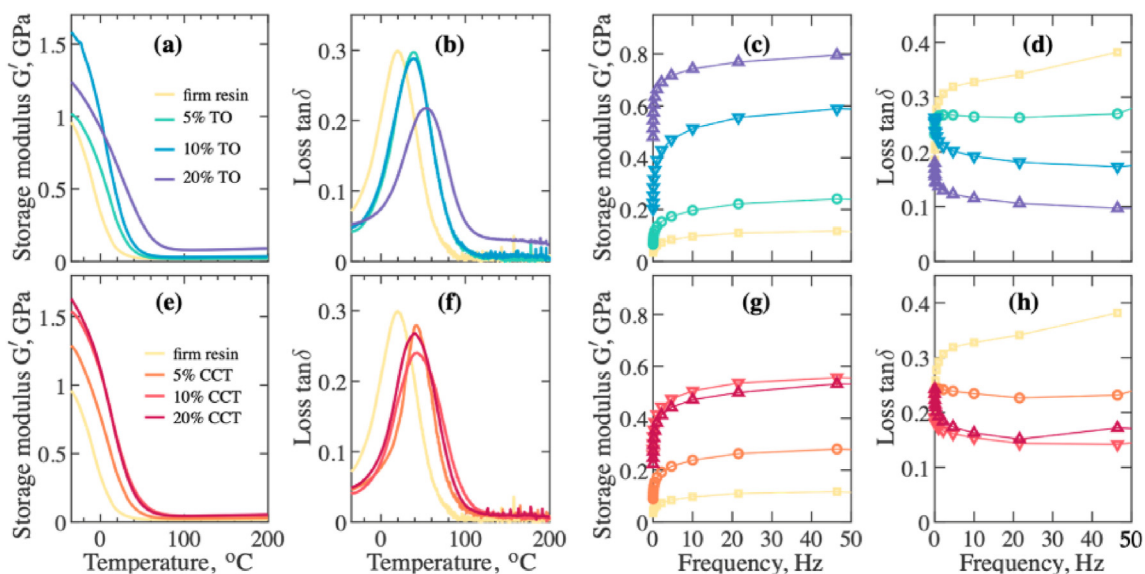


**Fig. 23 – Dynamic Mechanical Properties of Resin/TO composites (a-b) Storage Modulus & Loss Factor vs. Temperature (c-d) Storage Modulus & Loss Factor vs. Frequency. Dynamic Mechanical Properties of Resin/CCT composites (e-f) Storage Modulus & Loss Factor vs. Temperature (g-h) Storage Modulus & Loss Factor vs. Frequency (Reproduced with Permission from [103]).**

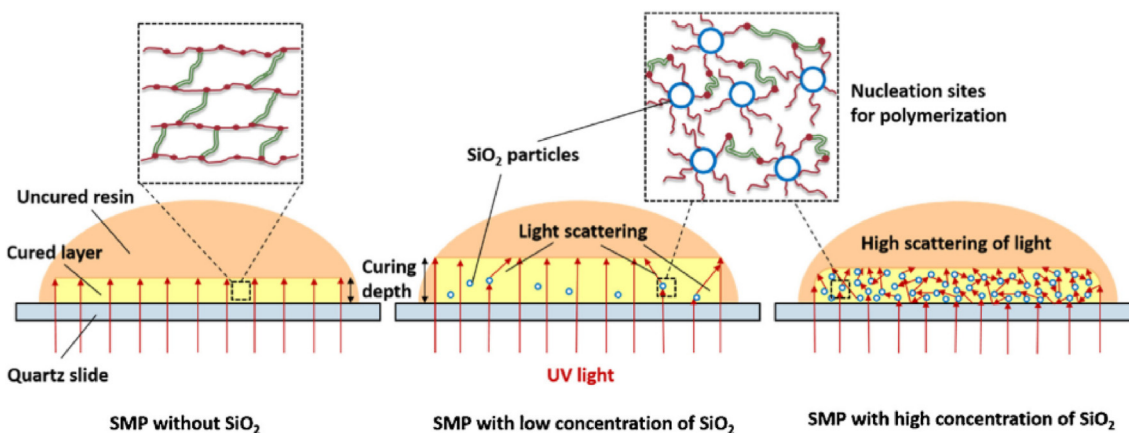


**Fig. 24 – Schematic diagram of phenomena involved in polymerization assistance due to nano-silica particles (Reproduced with Permission from [104]).**

methacrylate hydroxyapatite nanoparticle filler [105]. An improved polymer–particle interaction was achieved, in addition to the improved mechanical properties. Fabricated novel nanocomposites were found suitable for 3D printed bone structures, owing to achieved rheological property, wettability, degradation, and printability.

Epoxies are usually polymer monomers and are widely utilized for domestic applications, including epoxy floors and decoration. However, the utilization of these materials in mechanical applications requires their strength to be improved. Besides, novel processes for their processes could unleash their potential. Restrepo and Colorado [106] investigated magnetic reinforced epoxy composite through an innovative process termed direct ink writing (DIW), with varying contents. Different magnetite ratios with epoxy were

tested; 72:28 and 75:25 magnetite/epoxy composites were unfeasible due to higher magnetite concentrations, whereas 55:45 and 57:53 did not ensure the buildability of the material. Composite with 66% of magnetite was evaluated to be best in terms of repeatability of the AM process. It was concluded that higher magnetite contents provided better mechanical strength and microstructure. Manufactured composites provided superior mechanical strength even at lower reinforcement contents than pure epoxy and were found suitable for structural, thermal, and defense applications.

### 3.10. Hybrid polymers – based nanocomposites

To improve the desired properties of polymers, some researchers have attempted to produce hybrid polymer composites

comprising two polymer phases. Hybrid polymer composites result in the improvement of properties of the constituent with inferior properties. Fathi et al. [107] demonstrated the rapid manufacturing of bi-polymer composites, PCL-PDO, varying their relative content. Composite filaments were produced through an extruder following the chemical, mechanical and microstructural characterization experimentally and numerically. The feasibility of the AM process for bio-degradable composites could be a valuable tool for bio-implants. In vivo and ex vivo experiments revealed the materials' biocompatibility, and the material was found helpful to cell growth.

Carlson and Li [108] developed PLA-TPU composites with varying contents of both polymers. Stimuli-responsive materials were printed through FFF technology and were evaluated for response to temperature variations. Static and dynamic deformation was characterized along with the evaluation of the recovery process. Composites containing 80% PLA content were best in terms of consistency, recovery time, and shape memory characteristics.

Parsons et al. [109] fabricated composite filaments through extrusion for the FFF process with two different thermoplastic polymers, ABS and HDPE. Base polymers were incorporated with hollow glass spheres of different sizes and volume fractions. A theoretical model was also presented to predict the complex permittivity behavior and was successfully validated through experimental results. 3D printed samples revealed significantly low permittivity of the composites due to the incorporation of low permittivity glass spheres.

Chen et al. [110] produced a flexible TPU-rigid PLA blend with a 7:3 ratio to achieve robust mechanical properties. Polymer blend was further added with GO in varying content (up to 5 wt%). The authors reported the anisotropic behavior of 3D printed parts under tension and compression loading. 75.5% and 69.2% increase in tensile modulus and strength was observed at 0.5 wt% content of GO. Hybrid polymer nanocomposites also revealed the best cell growth in the biocompatibility test for the same GO concentration.

### 3.11. Shape memory polymer composites (SMPCs)

There has been an increasing interest in shape memory polymers (SMPs) to synthesize composites for functional applications. These materials can regain their original shape after deformation caused by any external stimuli. SMPs can be reinforced with nanoparticles to obtain shape memory nanocomposites with improved recovery mechanisms, mechanical properties, and controlled actuation. SMP composites have a massive potential for their applications in aerospace, biomedical, electronics, and 4D printing. Readers are referred to an interesting study by Xia et al. [111] on these materials and their applications.

Mulakkal et al. [112] developed cellulose-based hydrogel composites for 4DP. Carboxymethyl cellulose (CMC) hydrocolloid with incorporated cellulose pulp fibers resulted in around 50% volume fraction of reinforcement to hydrogel matrix with good dispersion. The extrusion process was used to fabricate the structures with controlled material deposition. The addition of MMT clay was also found beneficial in the storage stability of composites and the extrusion process. Likewise, Zhang et al. [113] investigated

the use of  $\text{Fe}_3\text{O}_4$  as reinforcement to PLA for 4DP applications. The magnetic field was employed to study the shape memory behavior of composites. 4D printed structures achieved their original shapes within few seconds. 4D printed bone-tissue structures were actuated using a magnetic field (27.5 kHz), and surface temperature was recorded around 40 °C. The testing of SMP composites revealed significant properties for their potential applications in the biomedical sector.

---

## 4. Applications

Applications of 3D printed polymer composites are discussed in this section. This section presents a summary of applications of different AM processes in various industrial sectors.

### 4.1. Biomedical sciences

AM processes are being rapidly employed in the biomedical field for tissue engineering and patient-specific implants. Different biomedical science materials include bio-inks, biomaterial inks, synthetic hydrogels, thermoplastic resins, ceramics, and metals. The materials for such applications must exhibit biocompatibility and significant mechanical properties [115]. Medical applications require implants, in most cases, with biocompatible materials, complex shapes, and a high degree of customization [5]. As discussed in previous sections, various materials are now tested to be safe and compatible with human tissues and the environment [68]. The complexity and customization, as these implants require patient-specific dimensions, can be achieved using AM processes [57]. Biocompatible scaffolds can be fabricated through FFF technology using bioactive materials as reinforcement to polymers [116]. In tissue engineering, precise control over porosity and fabrication of interconnected networks is quite challenging. FFF processes have been used for better dimensional and porosity control.

3D printed PLA/HA trabecular bone models, prepared by Wu et al. [58], displayed comparable mechanical strength compared to commonly used polymeric foam bone models. The wetting experiments performed on 3D printed PLA/HA composites revealed that the limiting contact angle could be reduced to 60° for a 30% mass fraction of HA in the PLA polymer matrix [57]. The tested material was found out to be biocompatible, and the synergistic effect of the two materials could provide alternative bone implant material to existing solutions. However, the print quality of the FFF process is a significant challenge to practical implementation. PCL/HA and PCL/SrHA 3D printed composites were tested for their biological performance and potential usage in bone tissue engineering applications (Fig. 25) [68]. *In-vitro* testing for composite scaffolds provided a ground for the biocompatibility of these materials. However, PCL/SrHA revealed better mineralization as compared to PCL/HA or pure PCL. Fathi et al. [107] demonstrated PCL-PDO composites' biocompatibility for the rapid fabrication of customized gastrointestinal stents. Successful *ex-vivo* and *in-vivo* experiments were performed on pig intestines (Fig. 26). Gayer et al. [66] recently developed a composite powder, from PLA and calcium carbonate, for the SLS

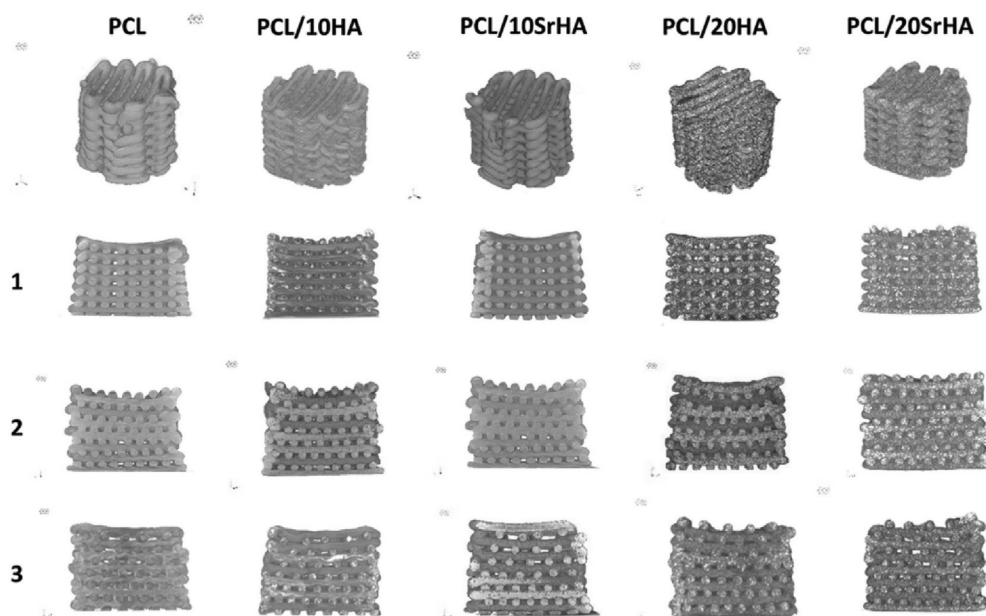


**Fig. 25 – 3D printed Sr-containing composite scaffolds for bone tissue engineering (Reproduced with Permission from [68]).**

process and successfully demonstrated the modified additive manufacturing system. Patient-specific bone implants were printed with interconnected pore-like structures; researchers also demonstrated newly developed material and fabrication methods for bone replacement implants with custom specifications.

Ongoing research also aims to adopt the bio-inspired design to the medical field to synthesize soft materials (polymers, rubber, and leather) that can be utilized for the fabrication of delicate organs and tissues. In this regard, AM would be a potential candidate for integration to realize advanced

materials [117]. Besides, research has also focused on the fabrication of smart materials for 4DP, which can change their shape over time, which has attracted biologists' and material scientists' attention for their potential use in biomedical applications [118]. Carve et al. [119] presented a review addressing the limitations and toxicity issues related to the rapid prototyping of complex monolithic devices produced using a vat polymerization process. It was concluded that applications of vat polymerization (VP) processes in biomedical engineering require in-depth research to eliminate the potential toxicity of the materials being used.



**Fig. 26 – Stent placement in perforated in-vivo pig intestines (Reproduced with Permission from [107]) (A) 3D-printed curved stents of 4 different sizes (B) An abdominal incision is made (C) A gastrointestinal incision is made, and a stent is placed. After stent placement, the intestinal incision was left partially open. Inset depicts the intestine before incision (D) The stent is secured in place with sutures, and the intestine is then placed back within the pig.**

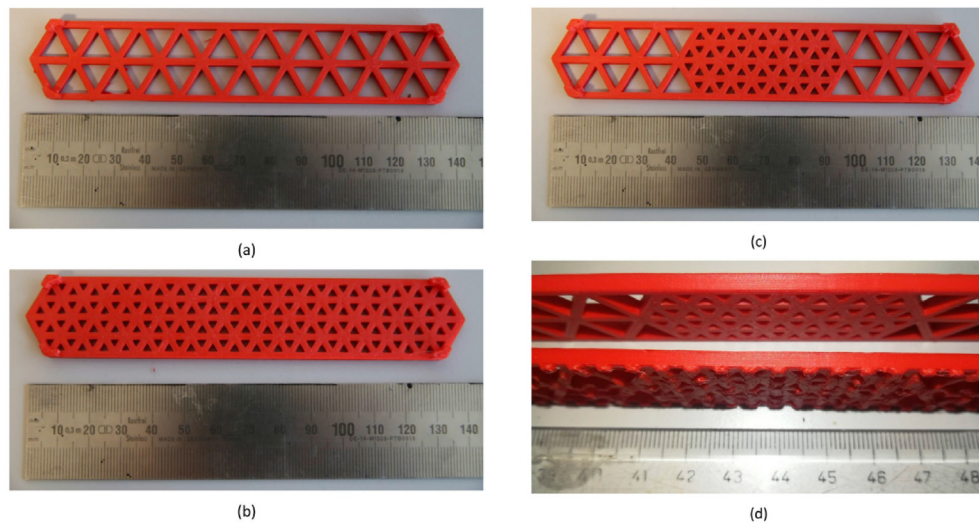


**Fig. 27 – 3D Printed reinforcements for Cementitious Composites with different internal structures (Reproduced with Permission from [128]).**

AM has found widespread use in biomaterials, regenerative medicine, tissue engineering, drug delivery, and laboratory device prototyping [120–122]. In the medical field, AM can also be used for aims such as teaching [123], functional flow modeling [124], procedural planning [125], and device engineering [123]. Although 3DP medical applications are still in early-stage, past and current studies show promising results and imply a bright future for the field. One of the main advantages of employing AM in the medical field is its ability to produce patient-specific devices and therapeutic approaches.

#### 4.2. Construction

The development of AM processes in the construction industry has recently urged researchers to develop novel materials, designs, and procedures due to limitations posed by the utilization of traditional construction materials in current AM processes [126,127]. Polymers and their composites are being considered as an alternative to conventional materials and reinforcements. Xu and Savija [128] developed a technique for the reinforcement of cementitious materials. 3D

printed ABS structures were utilized as reinforcements to conventionally casted fine-graded cement mortar (Fig. 27). Different reinforcement designs were printed and tested under uniaxial and 4-point loading conditions. Finite element simulations were also performed for 4-point tests. Results revealed that strain hardening behavior (desired for cementitious composites) could be achieved for specific reinforcement design, and improved tensile and flexural strengths were observed for structured polymer reinforced composites. Finite element simulation results also agreed well with experimental results. However, more sophisticated efforts must completely overcome the reinforcement issues and automation of the complete 3D concrete printing process. Salazar et al. [129] developed novel lattice structures for concrete reinforcement. Design structures were 3D printed using PLA and ABS polymer materials, following the filling of lattice structures with concrete (Fig. 28). The resulting structures revealed an improved ductility as compared to pure concrete with strain hardening behavior. Application of AM processes in construction has been hindered for several reasons,

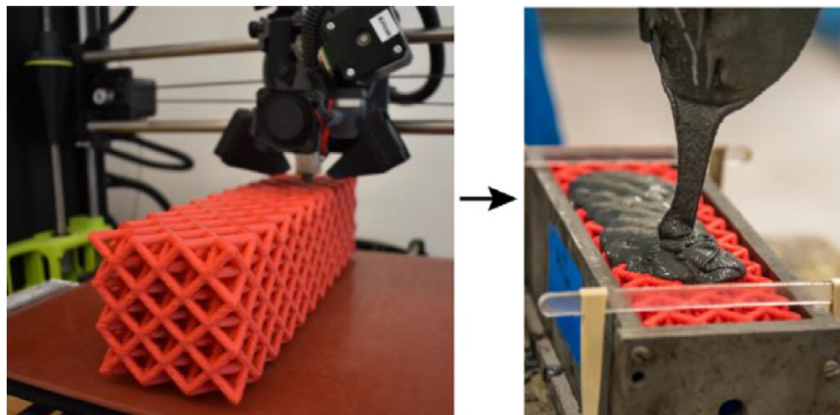


**Fig. 28 – Design and 3DP of lattice structures for concrete reinforcement (Reproduced with Permission from [129]).**

including introducing conventional reinforcements into 3D printed structures [12].

#### 4.3. Electrical/electronics

The outlook for producing advanced electronic components and systems using traditional manufacturing processes is grim, and such production might even be impossible. Therefore, AM processes are being utilized for cost-saving and environmentally friendly printed electronics [130]. AM techniques facilitate wide electronics applications, including the printing of resistors, capacitors, transistors, and circuits on a flexible substrate, as well as the production of flexible wearable gadgets [131] and a wide variety of mechanical, optical, electromagnetic, medical, and chemical sensors [132]. AM processes can fabricate micro-level monolithic devices; however, the applicability of these processes is limited, owing to materials' biocompatibility [119]. Researchers are also looking for strategies to print bioresorbable electronic devices for environmental sustainability [133].

Polymer composites responsive to the magnetic field are now widely employed in the electrical and electronics sectors [101]. PLA/carbon black composites manufactured by Beniak et al. [61] were investigated and proposed to be an appropriately conductive material for low voltage applications with significant mechanical strength. ABS/ZnFe<sub>2</sub>O<sub>4</sub> composites fabricated by Hamzah et al. [74] revealed improved mechanical, thermal, and electrical properties for high concentrations of ZnFe<sub>2</sub>O<sub>4</sub>. Although material electrical conductivity didn't increase much, the proposed material could still provide potential usage for low conductivity applications with significant mechanical strength. Titanium dioxide and calcium copper titanate polymer composites fabricated for the vat photopolymerization process revealed higher resolution, improved dielectric permittivity, and no dispersion at high frequencies. Materials with such properties could be utilized to manufacture electromagnetic devices operating at higher frequencies [103].

3D printing processes capture the interest in manufacturing telecommunication components with complex geometrical structures that are difficult, if not impossible, to realize with traditional manufacturing techniques. Clower et al. [134] performed the finite element analysis (FEA) of the Sierpinski antenna, which led to testing and evaluating its performance with 3D printed structures. Two different methodologies were adopted; 3D printing of polymer antenna following its coating with graphene nanoparticles, secondly, the 3D printing of polymer composites with embedded conducting particles. Although the fabricated antenna's conducting capacity was less than traditionally used copper material, the process provides rapid fabrication, lightweight structure, resistance against corrosion, and realization of complex geometrical systems.

Zhang et al. [135] explored shape memory polymers for their applications in photonics using 4D printing. 2 PP vat polymerization process was used, and around 300 nm of the resolution was achieved. Multiple colors were used to print nanoscale grids and analyzed for shape memory behavior. Extraordinary results were observed, as authors were able to recover original surfaces within seconds of heating.

#### 4.4. Mechanical Engineering

Typically, polymers exhibit inferior mechanical properties, thus limiting their direct utilization for structural or thermal applications. Therefore, different composites have been fabricated and tested for their mechanical and thermal performance. In this regard, HDPE/cardboard dust composites could be a sustainable and economical solution to low-cost engineering applications, where high strength is not required. These materials could be utilized in architectural/civil models, interior designing, and indoor paneling [70].

The utilization of 3DP processes in thermal sciences has gained attention owing to the opportunity of manufacturing complex geometries. Fabrication of complex shapes allows for a high volume-to-area ratio, which provides compact and efficient heat exchangers. Researchers are putting efforts into using numerical and experimental tools in evaluating the thermal performance of 3D printed polymer composites [136].

Likewise, PLA/CNF composites synthesized by Tekinalp et al. [64] provided an 80% and 200% increase in strength and elastic modulus, respectively, compared to pure PLA material. Tested materials were found suitable for robotic applications, even for low reinforcement percentages. 4D printed CNT reinforced PLA shape memory composites fabricated by Liu et al. [63] demonstrated their potential application for actuators based on significant shape memory force and shape recovery.

#### 4.5. Aerospace/defense

The aerospace industry has adopted AM processes to manufacture lightweight and high-performance polymer composite spare parts, as weight reduction in the aerospace industry leads to lower fuel consumption and cost savings [137]. There is a high degree of freedom for producing custom parts [138]. Therefore, this sector has undergone tremendous growth in terms of AM processes [139]. The deployment of AM processes in aerospace applications is growing swiftly. Different international standards have been developed by the German Institute for Standardization (DIN), the International Organization for Standardization (ISO), and the American Society for Testing and Materials (ASTM) to ensure the safe utilization of AM processes in the aerospace sector [140]. AM techniques are being used to manufacture jet engines and commercial plane parts, owing to the flexibility of the processes, the ability to design and realize complex structures with internal linings, customization of components, waste material reduction, multi-material utilization, and *in-situ* fabrication [141].

FFF can provide quicker and cheaper manufacturing of complex components of unmanned ariel vehicles (UAVs) [142]. Stratasys manufactured a jet engine UAV weighing only 33 pounds in collaboration with Aurora Flight Sciences [143]. Most of the parts for this lightweight UAV were fabricated through the FFF technique. Readers are also referred to [142] for more information on polymer composite UAVs. The anisotropy involved in AM processes and void contents makes their utilization challenging in the aerospace industry. If these challenges are successfully addressed, there is a massive scope of fuel and manufacturing cost saving in this sector [144].

AM processes could also serve the aim of customized and rapid fabrication in defense or the military. Most critical



applications in this sector require materials capable of remaining imperceptible under different frequencies. Therefore, efforts are being made to develop materials to serve such aims. Magnetite reinforced polymer-based composite materials can absorb different wavelengths. These materials can be utilized to manufacture submarines and drones to avoid radars [106]. Hollow glass spheres reinforced polymer composites manufactured by Parsons et al. [109] demonstrated very low dielectric constants for many frequencies. Such materials could also provide appealing applications in the military and defense sectors.

## 5. Challenges and future outlook

This article presents an up-to-date review of current trends, challenges, barriers, and research needs for AM of polymer nanocomposites and their applications in different sectors. It mainly aims to provide researchers with topical hindrances and limitations in AM of polymer nanocomposites. An extensive and comparative discussion is presented to address restrictions related to the processes and materials for AM of polymer nanocomposites.

### 5.1. Challenges and constraints

Based on the literature review, the challenges associated with materials and AM processes can be summarized as:

- A most critical requirement in feedstock material synthesis is the homogenous dispersion of reinforcement particles within the matrix, which plays a significant role in the composite's resulting properties [57]. Also, the accumulation of filler particles could affect the process, uncured photopolymer in the VP process, and the nozzle's clogging in the ME process. The uniform distribution is vital to achieving the required results and avoiding local stress concentrations, which result in product failure [101]. Nanoparticles play an influential role in improving mechanical properties; however, it comes at the cost of reduced ductility or failure strain in nanocomposites [48,60] due to poor interfacial adhesion and agglomeration of nanoparticles. The agglomerated nanoparticles act as stress concentrating defects, resulting in a deviation from expected material properties. Homogenous dispersion of nanoparticles is vital for optimum performance of the nanocomposites. A high-shear mixing process, like a twin-screw extruder, should be utilized to ensure adequate dispersion.
- The physical phenomena involved in AM process result in nanoparticles' alignment in the printing direction [86]. However, depending upon the functional application of nanocomposites, it could be beneficial to achieve improved electrical or thermal conductivity in the direction of oriented nanoparticles.
- Printing orientation strongly affects the mechanical properties of 3D printed nanocomposites. Anisotropic effects induced due to printing direction are widely reported [28,145]. The mechanical properties of vertically printed parts can reduce up to five times than the parts printed in XYZ direction. However, tailored mechanical properties with lower mechanical anisotropy can be achieved using a polymer blend [28].
- Nanoparticle loading alters the rheological properties of the polymer material, which in the molten state drives the successful AM process. The addition of nanoparticles to the polymer matrix restricts the polymer chains' mobility; besides, agglomeration also affects the rheological behavior, which affects the printability of the material.
- In the FFF process, the feedstock filament diameter plays a vital role in output product quality. Therefore, consistent filament diameter must be achieved during the filament extrusion process [57]. The choice of shape and size of reinforcement is critical as the particle's profile may not be suitable to provide good interfacial interaction between two phases [146]. The optimum particle shape and size must be chosen to avoid microstructural pores and localized stresses [106]. Many external and internal factors reported by Popescu et al. [18] also play a vital role in final product quality in the FFF process.
- The nature of filler material also affects its homogeneity within the composite matrix; polymers are generally hydrophobic. It is difficult, if not impossible, to mix a polymer solution with hydrophilic filler. Graphene, for example, can be dispersed using an aqueous suspension of nanofibrillated cellulose and so can be used in cellulose composites. Graphene has been proven to be an excellent filler material and promising for mechanical, thermal, and electrical applications. Therefore, it requires innovative approaches and processes for their proper utilization. The grafting of polymers has been demonstrated to be an effective method to improve dispersion [147]. However, there remain some challenges in the effective distribution of particles within the polymer matrices.
- The AM process's resolution plays an essential role in the final product's quality regarding its surface finish, higher resolution, dimensional tolerance, and mechanical strength. Generally, VP or PBF processes better control product surface morphology than ME processes, as it is convenient to control light source or powder particle size in VP and PBF processes, respectively. Sophisticated repeatability of the process can be achieved with higher resolutions, which would be beneficial even in critical engineering applications, e.g., synthetic bone models [58]. However, higher resolution usually means longer printing times. Thus, optimal process windows (3DP speed, temperature) and parameters need to be designed to coherently consider final product requirements, targeted cost, lead time, and starting polymer composite characteristics.
- Process conditions, including printing temperature, ambient temperature, infill pattern, infill density, and printing speed, significantly impact the printed part's properties [148]. Processes carried out under high temperatures would lead to fewer voids and porosity. The printability of material is an essential factor for consistent printing. Simple polymers can be printed conveniently; however, AM of composites is challenging for several reasons, such as gradients in temperature and flow characteristics of composite materials, as presented in previous sections.

- Polymer-reinforcement interaction corresponds to the composites' mechanical and adhesive properties and could also lead to structural defects [148]. This interaction can be enhanced through modified morphology, optimum aspect ratio, surface roughness, or by introducing functional groups to reinforcements. Increased interfacial bonding between the two phases will result in improved mechanical properties. Annealing has been utilized to improve interlayer adhesion of 3D printed composites [149]. However, detailed studies are still required to achieve optimum temperatures for different polymers or derive novel post-printing treatments.
- Reinforcement content or material composition directly impacts the final product's physical, mechanical, or thermal properties [150]. It is vital to determine the optimum polymer ratio to reinforce specific particle shape, size, and polymer type. The reliability of end products is tailored by the presence of structural defects, which still act as a significant limitation to high-performance applications [148]. Generally, structural defects can be avoided by carrying the process out in vacuum conditions [106]. However, this condition might not be the appropriate choice for low-cost applications. Furthermore, recycling waste material and end-life products must be considered during the design and manufacturing phase.

## 5.2. Future research directions

Research in material science and AM processes has urged scientists to quest for novel materials for functional applications, resulting in the synthesis of advanced nanocomposites with higher design flexibilities. It is worth mentioning that the AM processes should not be considered the full replacement to conventional manufacturing processes; instead, they can complement these processes for a synergic output. However, to utilize the advantages offered by AM processes, the designers must follow the design for AM (DfAM) approach. In this way, the interlinked parameters of process-material-design can serve several industries, including aerospace, automobiles, biomedical, and electrical, in a better way. The concluding remarks on future research directions are presented in Fig. 29 and also summarized as follows:

- **Novel Materials:** The synthesis of novel functional nanocomposites should keep on expanding the materials

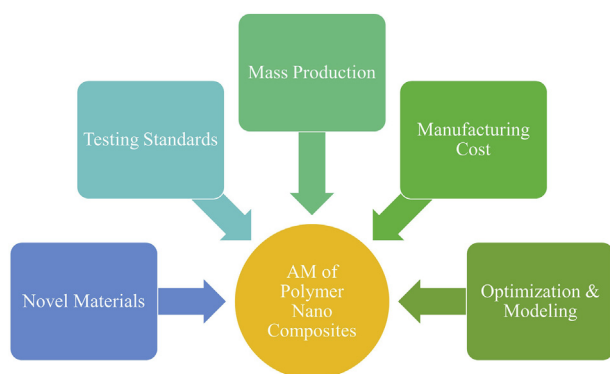


**Fig. 29 – Future research direction in AM of polymer nanocomposites.**

catalog. Nanocomposites for AM are limited, as very few polymers are explored yet. The search for more materials keeping in consideration the property-process-product relationship will further expand the compatibility of AM processes. Efforts should be made towards the utilization of natural reinforcements in polymer nanocomposites. Furthermore, only a few researchers attempted the AM process for bio-composites, which creates a considerable research gap in this area. AM of bio-composites will be a step forward to the utilization of sustainable materials.

- **Test Standards:** As mentioned in this review, plenty of parameters affect the printing process, making it unjust to compare AM parts properties with conventionally manufactured parts. Test standards considering the parameters involved in these processes should be developed to cater to the differences.
- **Mass Production:** The printing speed of these processes majorly limits their utilization for mass production. Heat transfer in FFF and residual stresses in PBF processes act as significant limitations to printing speeds. Although Big Area Additive Manufacturing (BAMM) scaled up the extrusion AM process with a 50 kg/h rate, it comes at lower resolution costs. Maintaining the printing resolution with adequate speed is still a major challenge.
- **Manufacturing Cost:** AM processes are economical for low volume production as tooling cost is eliminated. However, higher prices are associated with feedstock production for FFF or PBF processes. Some AM processes require post-processing, and the cost of energy consumption associated with lower speeds also adds up. Therefore, this point is somehow related to the mass production aspect.
- **Optimization & Modeling:** A major limitation prevails in predicting AM parts performance and optimization. The involvement of numerous printing parameters governing the final product quality cannot be optimized through oversimplified numerical simulation techniques. There is a need to develop optimization and modeling tools to correctly predict properties and optimize the functional parts for specific applications.

AM processes are relatively new-found than conventional manufacturing; therefore, several research areas are still active and under-explored. However, considering the current progress in material science and evolution of AM processes for nanocomposites, these methods and materials are expected to emerge as widely adopted in several industries.

## Declaration of Competing Interest

The authors declare that they have no known competing financial interests or personal relationships that could have appeared to influence the work reported in this paper.

## Acknowledgments

Open Access funding provided by the Qatar National Library (QNL).

## REFERENCES

- [1] Al Rashid A, Khalid MY, Imran R, Ali U, Koc M. Utilization of banana fiber-reinforced hybrid composites in the sports industry. *Materials (Basel)* 2020;13:3167. <https://doi.org/10.3390/ma13143167>.
- [2] Khalid MY, Al Rashid A, Arif ZU, Akram N, Arshad H, Garcia Marquez FP. Characterization of failure strain in fiber reinforced Composites : under on-Axis and off-Axis loading. *Crystals* 2021;11:216. <https://doi.org/10.3390/cryst11020216>.
- [3] Al Rashid A, Koc M. Creep and recovery behavior of continuous fiber-reinforced 3DP composites. *Polymers (Basel)* 2021;13:1644. <https://doi.org/10.3390/polym13101644>.
- [4] Yilmaz B, Al Rashid A, Ait Y, Evis Z, Koç M. Bioprinting : a review of processes , materials and applications. *Bioprinting* 2021;23:e00148. <https://doi.org/10.1016/j.bprint.2021.e00148>.
- [5] Ahangar P, Cooke ME, Weber MH, Rosenzweig DH. Current biomedical applications of 3D printing and additive manufacturing. *Appl Sci* 2019;9:1–23. <https://doi.org/10.3390/app9081713>.
- [6] Rane K, Strano M. A comprehensive review of extrusion-based additive manufacturing processes for rapid production of metallic and ceramic parts. *Adv Manuf* 2019;7:155–73. <https://doi.org/10.1007/s40436-019-00253-6>.
- [7] Nachal N, Moses JA, Karthik P, Anandharamakrishnan C. Applications of 3D printing in food processing. *Food Eng Rev* 2019;11:123–41. <https://doi.org/10.1007/s12393-019-09199-8>.
- [8] Khalid MY, Imran R, Arif ZU, Akram N, Arshad H, Al Rashid A, et al. Developments in chemical treatments , manufacturing techniques and potential applications of natural-fibers-based biodegradable composites. *Coatings* 2021;11:293. <https://doi.org/10.3390/coatings11030293>.
- [9] Adekanye SA, Mahamood RM, Akinlabi ET, Owolabi MG. Additive manufacturing: the future of manufacturing. *Mater Tehnol* 2017;51:709–15. <https://doi.org/10.17222/mit.2016.261>.
- [10] Wu H, Fahy WP, Kim S, Kim H, Zhao N, Pilato L, et al. Recent developments in polymers/polymer nanocomposites for additive manufacturing. *Prog Mater Sci* 2020;111. <https://doi.org/10.1016/j.pmatsci.2020.100638>.
- [11] Dontsov YV, Panin SV, Buslovich DG, Berto F. Taguchi optimization of parameters for feedstock fabrication and FDM manufacturing of wear-resistant UHMWPE-based composites. *Materials (Basel)* 2020;13:1–26. <https://doi.org/10.3390/ma13122718>.
- [12] Al Rashid A, Khan SA, G. Al-Ghamdi S, Koç M. Additive manufacturing: technology, applications, markets, and opportunities for the built environment. *Autom ConStruct* 2020;118:103268. <https://doi.org/10.1016/j.autcon.2020.103268>.
- [13] Gibson I, Rosen D, Stucker B. *Additive manufacturing technologies*. 2015. <https://doi.org/10.1007/978-1-4939-2113-3>. Springer.
- [14] Cullen AT, Price AD. Fabrication of 3D conjugated polymer structures via vat polymerization additive manufacturing. *Smart Mater Struct* 2019;28:104007. <https://doi.org/10.1088/1361-665x/ab35f1>.
- [15] Ngo TD, Kashani A, Imbalzano G, Nguyen KTQ, Hui D. Additive manufacturing (3D printing): a review of materials, methods, applications and challenges. *Compos B Eng* 2018;143:172–96. <https://doi.org/10.1016/j.compositesb.2018.02.012>.
- [16] Bernal PN, Delrot P, Loterie D, Li Y, Malda J, Moser C, et al. Volumetric bioprinting of complex living-tissue constructs within seconds. *Adv Mater* 2019;31. <https://doi.org/10.1002/adma.201904209>.
- [17] Chartrain NA, Williams CB, Whittington AR. A review on fabricating tissue scaffolds using vat photopolymerization. *Acta Biomater* 2018;74:90–111. <https://doi.org/10.1016/j.actbio.2018.05.010>.
- [18] Monneret S, Loubere V, Corbel S. Microstereolithography using a dynamic mask generator and a noncoherent visible light source. In: Courtois B, Crary SB, Ehrfeld W, Fujita H, Karam JM, Markus KW, editors. *Design, Test, and Microfabrication of MEMS/MOEMS*. vol. 3680; 1999. p. 553. <https://doi.org/10.1117/12.341246>. Paris, France.
- [19] Sun C, Fang N, Wu DM, Zhang X. Projection micro-stereolithography using digital micro-mirror dynamic mask. *Sensors Actuators A Phys* 2005;121:113–20. <https://doi.org/10.1016/j.sna.2004.12.011>.
- [20] Mou YA, Koc M. Dimensional capability of selected 3DP technologies. *Rapid Prototyp J* 2019;25:915–24. <https://doi.org/10.1108/RPJ-03-2019-0061>.
- [21] Xie R, Li D, Chao S. An inexpensive stereolithography technology with high power UV-LED light. *Rapid Prototyp J* 2011;17:441–50. <https://doi.org/10.1108/13552541111184170>.
- [22] Kim SH, Yeon YK, Lee JM, Chao JR, Lee YJ, Seo YB, et al. Precisely printable and biocompatible silk fibroin bioink for digital light processing 3D printing. *Nat Commun* 2018;9:1620. <https://doi.org/10.1038/s41467-018-03759-y>.
- [23] Manapat JZ, Chen Q, Ye P, Advincula RC. 3D printing of polymer nanocomposites via stereolithography. *Macromol Mater Eng* 2017;302:1600553. <https://doi.org/10.1002/mame.201600553>.
- [24] Ho CMB, Ng SH, Li KHH, Yoon Y-J. 3D printed microfluidics for biological applications. *Lab Chip* 2015;15:3627–37. <https://doi.org/10.1039/C5LC00685F>.
- [25] Karakurt I, Lin L. 3D printing technologies: techniques, materials, and post-processing. *Curr Opin Chem Eng* 2020;28:134–43. <https://doi.org/10.1016/j.coche.2020.04.001>.
- [26] Kelly BE, Bhattacharya I, Heidari H, Shusteff M, Spadaccini CM, Taylor HK. Volumetric additive manufacturing via tomographic reconstruction. *Science* 2019;363:1075–9. <https://doi.org/10.1126/science.aau7114>.
- [27] Moriche R, Artigas J, Reigosa L, Sánchez M, Prolongo SG, Ureña A. Modifications induced in photocuring of Bis-GMA/TEGDMA by the addition of graphene nanoplatelets for 3D printable electrically conductive nanocomposites. *Compos Sci Technol* 2019;184. <https://doi.org/10.1016/j.compscitech.2019.107876>.
- [28] Torrado AR, Shemelya CM, English JD, Lin Y, Wicker RB, Roberson DA. Characterizing the effect of additives to ABS on the mechanical property anisotropy of specimens fabricated by material extrusion 3D printing. *Addit Manuf* 2015;6:16–29. <https://doi.org/10.1016/j.addma.2015.02.001>.
- [29] Diegel O, Nordin A, Motte D. *Additive manufacturing technologies. A pract. Guid. To des. Addit. Manuf.*. Singapore: Springer Singapore; 2019. p. 19–39. [https://doi.org/10.1007/978-981-13-8281-9\\_2](https://doi.org/10.1007/978-981-13-8281-9_2).
- [30] Jiang J, Xu X, Stringer J. Support structures for additive manufacturing: a review. *J Manuf Mater Process* 2018;2:64. <https://doi.org/10.3390/jmmp2040064>.
- [31] Turner B N, Strong R, Gold S A. A review of melt extrusion additive manufacturing processes: I. Process design and modeling. *Rapid Prototyp J* 2014;20:192–204. <https://doi.org/10.1108/RPJ-01-2013-0012>.
- [32] Dikshit V, Nagalingam AP, Yap YL, Sing SL, Yeong WY, Wei J. Crack monitoring and failure investigation on inkjet printed sandwich structures under quasi-static indentation test. *Mater Des* 2018;137:140–51. <https://doi.org/10.1016/j.matdes.2017.10.014>.

- [33] Popescu D, Zapciu A, Amza C, Baci F, Marinescu R. FDM process parameters influence over the mechanical properties of polymer specimens: a review. *Polym Test* 2018;69:157–66. <https://doi.org/10.1016/j.polymertesting.2018.05.020>.
- [34] Jiang J, Lou J, Hu G. Effect of support on printed properties in fused deposition modelling processes. *Virtual Phys Prototyp* 2019;14:308–15. <https://doi.org/10.1080/17452759.2019.1568835>.
- [35] Goh GD, Yap YL, Tan HKJ, Sing SL, Goh GL, Yeong WY. Process–structure–properties in polymer additive manufacturing via material extrusion: a review. *Crit Rev Solid State Mater Sci* 2020;45:113–33. <https://doi.org/10.1080/10408436.2018.1549977>.
- [36] Ahn S, Montero M, Odell D, Roundy S, Wright PK. Anisotropic material properties of fused deposition modeling {ABS}. *Rapid Prototyp J* 2002;8:248–57. <https://doi.org/10.1108/13552540210441166>.
- [37] Tsai C-Y, Cheng C-W, Lee A-C, Tsai M-C. Synchronized multi-spot scanning strategies for the laser powder bed fusion process. *Addit Manuf* 2019;27:1–7. <https://doi.org/10.1016/j.ADDMA.2019.02.009>.
- [38] Nakano T, Ishimoto T. Powder-based additive manufacturing for development of tailor-made implants for orthopedic applications. *KONA Powder Part J* 2015;32:75–84. <https://doi.org/10.14356/kona.2015015>.
- [39] Beaman JJ, Deckard CR. *Selective laser sintering with assisted powder handling*. Google Patents 1990:17.
- [40] Kruth J, Mercelis P, Van Vaerenbergh J, Froyen L, Rombouts M. Binding mechanisms in selective laser sintering and selective laser melting. *Rapid Prototyp J* 2005;11:26–36. <https://doi.org/10.1108/13552540510573365>.
- [41] Tolochko NK, Khlopkov YV, Mozzharov SE, Ignatiev MB, Laoui T, Titov VI. Absorptance of powder materials suitable for laser sintering. *Rapid Prototyp J* 2000;6:155–61. <https://doi.org/10.1108/13552540010337029>.
- [42] Li L. Advances and characteristics of high-power diode laser materials processing. *Opt Laser Eng* 2000;34:231–53. [https://doi.org/10.1016/S0143-8166\(00\)00066-X](https://doi.org/10.1016/S0143-8166(00)00066-X).
- [43] Kalms M, Narita R, Thomy C, Vollertsen F, Bergmann RB. New approach to evaluate 3D laser printed parts in powder bed fusion-based additive manufacturing in-line within closed space. *Addit Manuf* 2019;26:161–5. <https://doi.org/10.1016/j.addma.2019.01.011>.
- [44] Abdullah A. Controlling the porosity of 316L stainless steel parts manufactured via the powder bed fusion process. *Rapid Prototyp J* 2019;25:162–75. <https://doi.org/10.1108/RPJ-11-2017-0226>.
- [45] Bourbigot S, Duquesne S, Jama C. Polymer nanocomposites: how to reach low flammability? *Macromol Symp* 2006;233:180–90. <https://doi.org/10.1002/masy.200690016>.
- [46] Paul DR, Robeson LM. Polymer nanotechnology: nanocomposites. *Polymer (Guildf)* 2008;49:3187–204. <https://doi.org/10.1016/j.polymer.2008.04.017>.
- [47] Meng S, He H, Jia Y, Yu P, Huang B, Chen J. Effect of nanoparticles on the mechanical properties of acrylonitrile–butadiene–styrene specimens fabricated by fused deposition modeling. *J Appl Polym Sci* 2017;134. <https://doi.org/10.1002/app.44470>.
- [48] Weng Z, Wang J, Senthil T, Wu L. Mechanical and thermal properties of ABS/montmorillonite nanocomposites for fused deposition modeling 3D printing. *Mater Des* 2016;102:276–83. <https://doi.org/10.1016/j.matdes.2016.04.045>.
- [49] Francis V, Jain PK. Achieving improved dielectric, mechanical, and thermal properties of additive manufactured parts via filament modification using OMMT-based nanocomposite. *Prog Addit Manuf* 2017;2:109–15. <https://doi.org/10.1007/s40964-017-0031-1>.
- [50] Kim K, Park J, Suh J hoon, Kim M, Jeong Y, Park I. 3D printing of multiaxial force sensors using carbon nanotube (CNT)/thermoplastic polyurethane (TPU) filaments. *Sensors Actuators, A Phys* 2017;263:493–500. <https://doi.org/10.1016/j.sna.2017.07.020>.
- [51] Christ JF, Aliheidari N, Ameli A, Pötschke P. 3D printed highly elastic strain sensors of multiwalled carbon nanotube/thermoplastic polyurethane nanocomposites. *Mater Des* 2017;131:394–401. <https://doi.org/10.1016/j.matdes.2017.06.011>.
- [52] Kwok SW, Goh KHH, Tan ZD, Tan STM, Tjiu WW, Soh JY, et al. Electrically conductive filament for 3D-printed circuits and sensors. *Appl Mater Today* 2017;9:167–75. <https://doi.org/10.1016/j.apmt.2017.07.001>.
- [53] Dul S, Fambri L, Pegoretti A. Fused deposition modelling with ABS-graphene nanocomposites. *Compos Part A Appl Sci Manuf* 2016;85:181–91. <https://doi.org/10.1016/j.compositesa.2016.03.013>.
- [54] Carrasco F, Pagès P, Gámez-Pérez J, Santana OO, Maspoch ML. Processing of poly(lactic acid): characterization of chemical structure, thermal stability and mechanical properties. *Polym Degrad Stab* 2010;95:116–25. <https://doi.org/10.1016/j.polymdegradstab.2009.11.045>.
- [55] Zhang Q, Lei H, Cai H, Han X, Lin X, Qian M, et al. Improvement on the properties of microcrystalline cellulose/polylactic acid composites by using activated biochar. *J Clean Prod* 2020;252:119898. <https://doi.org/10.1016/j.jclepro.2019.119898>.
- [56] Tian X, Liu T, Wang Q, Dilmurat A, Li D, Ziegmann G. Recycling and remanufacturing of 3D printed continuous carbon fiber reinforced PLA composites. *J Clean Prod* 2017;142:1609–18. <https://doi.org/10.1016/j.jclepro.2016.11.139>.
- [57] Petrovskaya TS, Toropkov NE, Mironov EG, Azarmi F. 3D printed biocompatible polylactide-hydroxyapatite based material for bone implants. *Mater Manuf Process* 2018;33:1899–904. <https://doi.org/10.1080/10426914.2018.1476764>.
- [58] Wu D, Spanou A, Diez-Escudero A, Persson C. 3D-printed PLA/HA composite structures as synthetic trabecular bone: a feasibility study using fused deposition modeling. *J Mech Behav Biomed Mater* 2020;103:103608. <https://doi.org/10.1016/j.jmbbm.2019.103608>.
- [59] Backes EH, Pires LDN, Beatrice CAG, Costa LC, Passador FR, Pessan LA. Fabrication of biocompatible composites of poly(lactic acid)/hydroxyapatite envisioning medical applications. *Polym Eng Sci* 2020;60:636–44. <https://doi.org/10.1002/pen.25322>.
- [60] Coppola B, Cappetti N, Di Maio L, Scarfato P, Incarnato L. Layered silicate reinforced polylactic acid filaments for 3D printing of polymer nanocomposites. In: 2017 IEEE 3rd Int. Forum res. Technol. Soc. Ind.; 2017. p. 1–4. <https://doi.org/10.1109/RTSI.2017.8065892>.
- [61] Beniak J, Krizan P, Matus M. Conductive material properties for fdm additive manufacturing. *MM Sci J* 2020;2020:3846–51. [https://doi.org/10.17973/MMSJ.2020\\_03\\_2019135](https://doi.org/10.17973/MMSJ.2020_03_2019135).
- [62] Mora A, Verma P, Kumar S. Electrical conductivity of CNT/polymer composites: 3D printing, measurements and modeling. *Compos B Eng* 2020;183:107600. <https://doi.org/10.1016/j.compositesb.2019.107600>.
- [63] Liu Y, Zhang W, Zhang F, Leng J, Pei S, Wang L, et al. Microstructural design for enhanced shape memory behavior of 4D printed composites based on carbon nanotube/polylactic acid filament. *Compos Sci Technol*

- 2019;181:107692. <https://doi.org/10.1016/j.compscitech.2019.107692>.
- [64] Tekinalp HL, Meng X, Lu Y, Kunc V, Love LJ, Peter WH, et al. High modulus biocomposites via additive manufacturing: cellulose nanofibril networks as “microsponges. *Compos B Eng* 2019;173:106817. <https://doi.org/10.1016/j.compositesb.2019.05.028>.
- [65] Zhang D, Chi B, Li B, Gao Z, Du Y, Guo J, et al. Fabrication of highly conductive graphene flexible circuits by 3D printing. *Synth Met* 2016;217:79–86. <https://doi.org/10.1016/j.synthmet.2016.03.014>.
- [66] Gayer C, Ritter J, Bullemer M, Grom S, Jauer L, Meiners W, et al. Development of a solvent-free polylactide/calcium carbonate composite for selective laser sintering of bone tissue engineering scaffolds. *Mater Sci Eng C* 2019;101:660–73. <https://doi.org/10.1016/j.msec.2019.03.101>.
- [67] Mellor LF, Huebner P, Cai S, Mohiti-Asli M, Taylor MA, Spang J, et al. Fabrication and evaluation of electrospun, 3D-bioprinted, and combination of electrospun/3D-bioprinted scaffolds for tissue engineering applications. *BioMed Res Int* 2017;2017. <https://doi.org/10.1155/2017/6956794>.
- [68] Pierantozzi D, Scalzone A, Jindal S, Stpniece L, Šalma-Ancane K, Dalgarno K, et al. 3D printed Sr-containing composite scaffolds: effect of structural design and material formulation towards new strategies for bone tissue engineering. *Compos Sci Technol* 2020;191. <https://doi.org/10.1016/j.compscitech.2020.108069>.
- [69] Tahmasebinia F, Niemelä M, Sepasgozar SME, Lai TY, Su W, Reddy KR, et al. Three-dimensional printing using recycled high-density polyethylene: technological challenges and future directions for construction. *Buildings* 2018;8. <https://doi.org/10.3390/buildings8110165>.
- [70] Gregor-Sveteč D, Leskovšek M, Vrabčič Brodnjak U, Stanković Elesini U, Muck D, Urbas R. Characteristics of HDPE/cardboard dust 3D printable composite filaments. *J Mater Process Technol* 2020;276:116379. <https://doi.org/10.1016/j.jmatprotec.2019.116379>.
- [71] Palmero EM, Casaleiz D, de Vicente J, Hernández-Vicen J, López-Vidal S, Ramiro E, et al. Composites based on metallic particles and tuned filling factor for 3D-printing by Fused Deposition Modeling. *Compos Part A Appl Sci Manuf* 2019;124:105497. <https://doi.org/10.1016/j.compositesa.2019.105497>.
- [72] Kulich DM, Gaggar SK, Lowry V, Stepien R. Acrylonitrile–butadiene–styrene (ABS) polymers. *Kirk-Othmer encycl. Chem. Technol*, American Cancer Society. 2003. <https://doi.org/10.1002/0471238961.01021911211209.a01.pub2>.
- [73] Cress AK, Huynh J, Anderson EH, O’neill R, Schneider Y, Keleş Ö. Effect of recycling on the mechanical behavior and structure of additively manufactured acrylonitrile butadiene styrene (ABS). *J Clean Prod* 2021;279:123689. <https://doi.org/10.1016/j.jclepro.2020.123689>.
- [74] Hamzah KA, Yeoh CK, Mohd Noor M, Teh PL, Sazali SA, Aw YY, et al. Effect of the printing orientation on the mechanical properties and thermal and electrical conductivity of ABS-ZnFe<sub>2</sub>O<sub>4</sub> composites. *J Mater Eng Perform* 2019;28:5860–8. <https://doi.org/10.1007/s11665-019-04313-7>.
- [75] Chizari K, Daoud MA, Ravindran AR, Therriault D. 3D printing of highly conductive nanocomposites for the functional optimization of liquid sensors. *Small* 2016;12:6076–82. <https://doi.org/10.1002/smll.201601695>.
- [76] Dorigato A, Moretti V, Dul S, Unterberger SH, Pegoretti A. Electrically conductive nanocomposites for fused deposition modelling. *Synth Met* 2017;226:7–14. <https://doi.org/10.1016/j.synthmet.2017.01.009>.
- [77] Dul S, Fambri L, Pegoretti A. Filaments production and fused deposition modelling of ABS/carbon nanotubes composites. *Nanomaterials* 2018;8. <https://doi.org/10.3390/nano8010049>.
- [78] Yamamoto BE, Trimble AZ, Minei B, Ghasemi Nejhad MN. Development of multifunctional nanocomposites with 3-D printing additive manufacturing and low graphene loading. *J Thermoplast Compos Mater* 2019;32:383–408. <https://doi.org/10.1177/0892705718759390>.
- [79] Momenzadeh N, Miyajima H, Berfield TA. Influences of zirconium tungstate additives on characteristics of polyvinylidene fluoride (PVDF) components fabricated via material extrusion additive manufacturing process. *Int J Adv Manuf Technol* 2019;103:4713–20. <https://doi.org/10.1007/s00170-019-03978-7>.
- [80] Kim H, Islam MT, Md Didarul I, Chavez LA, Garcia Rosales CA, Wilburn BR, et al. Increased piezoelectric response in functional nanocomposites through multiwall carbon nanotube interface and fused-deposition modeling three-dimensional printing. *MRS Commun* 2017;7:960–6. <https://doi.org/10.1557/mrc.2017.126>.
- [81] Chen R, Morsi Y, Patel S, Ke Q, Mo X. A novel approach via combination of electrospinning and FDM for tri-leaflet heart valve scaffold fabrication. *Front Mater Sci China* 2009;3:359–66. <https://doi.org/10.1007/s11706-009-0067-3>.
- [82] Hohimer C, Aliheidari N, Mo C, Ameli A. In: Mechanical behavior of 3D printed multiwalled carbon nanotube/thermoplastic Polyurethane nanocomposites, Vol 1; 2017. <https://doi.org/10.1115/SMASIS2017-3808>.
- [83] Gnanasekaran K, Heijmans T, van Bennekom S, Woldhuis H, Wijnia S, de With G, et al. 3D printing of CNT- and graphene-based conductive polymer nanocomposites by fused deposition modeling. *Appl Mater Today* 2017;9:21–8. <https://doi.org/10.1016/j.apmt.2017.04.003>.
- [84] Zhu W, Yan C, Shi Y, Wen S, Liu J, Wei Q, et al. A novel method based on selective laser sintering for preparing high-performance carbon fibres/polyamide 12/epoxy ternary composites. *Sci Rep* 2016;6:1–10. <https://doi.org/10.1038/srep33780>.
- [85] Salazar A, Rico A, Rodríguez J, Segurado Escudero J, Seltzer R, Martín de la Escalera Cutillas F. Monotonic loading and fatigue response of a bio-based polyamide PA11 and a petrol-based polyamide PA12 manufactured by selective laser sintering. *Eur Polym J* 2014;59:36–45. <https://doi.org/10.1016/j.eurpolymj.2014.07.016>.
- [86] Zhu D, Ren Y, Liao G, Jiang S, Liu F, Guo J, et al. Thermal and mechanical properties of polyamide 12/graphene nanoplatelets nanocomposites and parts fabricated by fused deposition modeling. *J Appl Polym Sci* 2017;134:1–13. <https://doi.org/10.1002/app.45332>.
- [87] O’ Connor HJ, Dowling DP. Comparison between the properties of polyamide 12 and glass bead filled polyamide 12 using the multi jet fusion printing process. *Addit Manuf* 2020;31:100961. <https://doi.org/10.1016/j.addma.2019.100961>.
- [88] Chunze Y, Yusheng S, Jinsong Y, Jinhui L. A nanosilica/nylon-12 composite powder for selective laser sintering. *J Reinforc Plast Compos* 2009;28:2889–902. <https://doi.org/10.1177/0731684408094062>.
- [89] Athreya SR, Kalaitzidou K, Das S. Processing and characterization of a carbon black-filled electrically conductive Nylon-12 nanocomposite produced by selective laser sintering. *Mater Sci Eng, A* 2010;527:2637–42. <https://doi.org/10.1016/j.msea.2009.12.028>.
- [90] Salmoria GV, Paggi RA, Lago A, Beal VE. Microstructural and mechanical characterization of PA12/MWCNTs nanocomposite manufactured by selective laser sintering.

- Polym Test 2011;30:611–5. <https://doi.org/10.1016/j.polymertesting.2011.04.007>.
- [91] Goodridge RD, Shofner ML, Hague RJM, McClelland M, Schlea MR, Johnson RB, et al. Processing of a Polyamide-12/carbon nanofibre composite by laser sintering. *Polym Test* 2011;30:94–100. <https://doi.org/10.1016/j.polymertesting.2010.10.011>.
- [92] Koo JH, Lao S, Ho W, Ngyuen K, Cheng J, Pilato L, et al. Polyamide nanocomposites for selective laser sintering. In: 17th solid free. Fabr. Symp. SFF 2006; 2006. p. 392–409.
- [93] Cheng J, Lao S, Nguyen K, Ho W, Cummings A, Koo J. SLS processing studies of nylon 11 nanocomposites. *Proc Int Solid Free Fabr Symp* 2005:141–9.
- [94] Moore AL, Cummings AT, Jensen JM, Shi L, Koo JH. Thermal conductivity measurements of nylon 11-carbon nanofiber nanocomposites. *J Heat Tran* 2009;131. <https://doi.org/10.1115/1.3139110>.
- [95] Warnakula A, Singamneni S. Selective laser sintering of nano Al<sub>2</sub>O<sub>3</sub> infused polyamide. *Materials (Basel)* 2017;10. <https://doi.org/10.3390/ma10080864>.
- [96] Zheng H, Zhang J, Lu S, Wang G, Xu Z. Effect of core-shell composite particles on the sintering behavior and properties of nano-Al<sub>2</sub>O<sub>3</sub>/polystyrene composite prepared by SLS. *Mater Lett* 2006;60:1219–23. <https://doi.org/10.1016/j.matlet.2005.11.003>.
- [97] Wilts EM, Pekkanen AM, White BT, Meenakshisundaram V, Aduba DC, Williams CB, et al. Vat photopolymerization of charged monomers: 3D printing with supramolecular interactions. *Polym Chem* 2019;10:1442–51. <https://doi.org/10.1039/C8PY01792A>.
- [98] Mohan D, Sajab MS, Kaco H, Bakarudin SB, Noor AM. 3D printing of uv-curable polyurethane incorporated with surface-grafted nanocellulose. *Nanomaterials* 2019;9. <https://doi.org/10.3390/nano9121726>.
- [99] Esposito Corcione C, Striani R, Montagna F, Cannoletta D. Organically modified montmorillonite polymer nanocomposites for stereolithography building process. *Polym Adv Technol* 2015;26:92–8. <https://doi.org/10.1002/pat.3425>.
- [100] Weng Z, Zhou Y, Lin W, Senthil T, Wu L. Structure-property relationship of nano enhanced stereolithography resin for desktop SLA 3D printer. *Compos Part A Appl Sci Manuf* 2016;88:234–42. <https://doi.org/10.1016/j.compositesa.2016.05.035>.
- [101] Nagarajan B, Arshad M, Ullah A, Mertiny P, Qureshi AJ. Additive manufacturing ferromagnetic polymers using stereolithography – materials and process development. *Manuf Lett* 2019;21:12–6. <https://doi.org/10.1016/j.mfglet.2019.06.003>.
- [102] Lu L, Zhang Z, Xu J, Pan Y. 3D-printed polymer composites with acoustically assembled multidimensional filler networks for accelerated heat dissipation. *Compos B Eng* 2019;174. <https://doi.org/10.1016/j.compositesb.2019.106991>.
- [103] Malas A, Isakov D, Couling K, Gibbons GJ. Fabrication of high permittivity resin composite for vat photopolymerization 3D printing: morphology, thermal, dynamic mechanical and dielectric properties. *Materials (Basel)* 2019;12. <https://doi.org/10.3390/ma122333818>.
- [104] Choong YYC, Maleksaedi S, Eng H, Yu S, Wei J, Su PC. High speed 4D printing of shape memory polymers with nanosilica. *Appl Mater Today* 2020;18:100515. <https://doi.org/10.1016/j.apmt.2019.100515>.
- [105] Yang Y, Zhang Q, Xu T, Zhang H, Zhang M, Lu L, et al. Photocrosslinkable nanocomposite ink for printing strong, biodegradable and bioactive bone graft. *Biomaterials* 2020;263. <https://doi.org/10.1016/j.biomaterials.2020.120378>.
- [106] Restrepo JJ, Colorado HA. Additive manufacturing of composites made of epoxy resin with magnetite particles fabricated with the direct ink writing technique. *J Compos Mater* 2020;54:647–57. <https://doi.org/10.1177/0021998319865019>.
- [107] Fathi P, Capron G, Tripathi I, Misra S, Ostadhossein F, Selmic L, et al. Computed tomography-guided additive manufacturing of Personalized Absorbable Gastrointestinal Stents for intestinal fistulae and perforations. *Biomaterials* 2020;228:119542. <https://doi.org/10.1016/j.biomaterials.2019.119542>.
- [108] Carlson M, Li Y. Development and kinetic evaluation of a low-cost temperature-sensitive shape memory polymer for 4-dimensional printing. *Int J Adv Manuf Technol* 2020;106:4263–79. <https://doi.org/10.1007/s00170-020-04927-5>.
- [109] Parsons P, Larimore Z, Muhammed F, Mirotznik M. Fabrication of low dielectric constant composite filaments for use in fused filament fabrication 3D printing. *Addit Manuf* 2019;30:100888. <https://doi.org/10.1016/j.addma.2019.100888>.
- [110] Chen Q, Mangadiao JD, Wallat J, De Leon A, Pokorski JK, Advincula RC. 3D printing biocompatible polyurethane/poly(lactic acid)/graphene oxide nanocomposites: anisotropic properties. *ACS Appl Mater Interfaces* 2017;9:4015–23. <https://doi.org/10.1021/acsami.6b11793>.
- [111] Xia Y, He Y, Zhang F, Liu Y, Leng J. A review of shape memory polymers and composites: mechanisms, materials, and applications. *Adv Mater* 2021;33:1–33. <https://doi.org/10.1002/adma.202000713>.
- [112] Mulakkal MC, Trask RS, Ting VP, Seddon AM. Responsive cellulose-hydrogel composite ink for 4D printing. *Mater Des* 2018;160:108–18. <https://doi.org/10.1016/j.matdes.2018.09.009>.
- [113] Zhang F, Wang L, Zheng Z, Liu Y, Leng J. Magnetic programming of 4D printed shape memory composite structures. *Compos Part A Appl Sci Manuf* 2019;125:105571. <https://doi.org/10.1016/j.compositesa.2019.105571>.
- [114] Wei X, Li D, Jiang W, Gu Z, Wang X, Zhang Z, et al. 3D printable graphene composite. *Sci Rep* 2015;5:1–7. <https://doi.org/10.1038/srep11181>.
- [115] Dávila JL, Freitas MS, Inforçatti Neto P, Silveira ZC, Silva JVL, d'Ávila MA. Fabrication of PCL/β-TCP scaffolds by 3D mini-screw extrusion printing. *J Appl Polym Sci* 2016;133. <https://doi.org/10.1002/app.43031>.
- [116] Kumar S, Kruth JP. Composites by rapid prototyping technology. *Mater Des* 2010;31:850–6. <https://doi.org/10.1016/j.matdes.2009.07.045>.
- [117] Li S, Bai H, Shepherd RF, Zhao H. Bio-inspired design and additive manufacturing of soft materials, machines, robots, and haptic interfaces. *Angew Chem Int Ed* 2019;58:11182–204. <https://doi.org/10.1002/anie.201813402>.
- [118] González-Henríquez CM, Sarabia-Vallejos MA, Rodríguez-Hernández J. Polymers for additive manufacturing and 4D-printing: materials, methodologies, and biomedical applications. *Prog Polym Sci* 2019;94:57–116. <https://doi.org/10.1016/j.progpolymsci.2019.03.001>.
- [119] Carve M, Wlodkowic D. 3D-printed chips: compatibility of additive manufacturing photopolymeric substrata with biological applications. *Micromachines* 2018;9. <https://doi.org/10.3390/mi9020091>.
- [120] Gross BC, Erkal JL, Lockwood SY, Chen C, Spence DM. Evaluation of 3D printing and its potential impact on biotechnology and the chemical sciences. *Anal Chem* 2014;86:3240–53. <https://doi.org/10.1021/ac403397r>.
- [121] Vukicevic M, Mosadegh B, Min JK, Little SH. Cardiac 3D printing and its future directions. *JACC Cardiovasc Imaging* 2017;10:171–84. <https://doi.org/10.1016/j.jcmg.2016.12.001>.
- [122] Krujatz F, Lode A, Seidel J, Bley T, Gelinsky M, Steingroewer J. Additive Biotech—chances, challenges, and recent applications of additive manufacturing technologies

- in biotechnology. *N Biotech* 2017;39:222–31. <https://doi.org/10.1016/j.nbt.2017.09.001>.
- [123] Suzuki M, Ogawa Y, Kawano A, Hagiwara A, Yamaguchi H, Ono H. Rapid prototyping of temporal bone for surgical training and medical education. *Acta Otolaryngol* 2004;124:400–2. <https://doi.org/10.1080/00016480410016478>.
- [124] Mahmood F, Owais K, Montealegre-Gallegos M, Matyal R, Panzica P, Maslow A, et al. Echocardiography derived three-dimensional printing of normal and abnormal mitral annuli. *Ann Card Anaesth* 2014;17:279. <https://doi.org/10.4103/0971-9784.142062>.
- [125] Valverde I, Gomez G, Coserria JF, Suarez-Mejias C, Uribe S, Sotelo J, et al. 3D printed models for planning endovascular stenting in transverse aortic arch hypoplasia: 3D Cardiovascular Model Simulation. *Cathet Cardiovasc Interv* 2015;85:1006–12. <https://doi.org/10.1002/ccd.25810>.
- [126] Panda B, Paul SC, Hui LJ, Tay YWD, Tan MJ. Additive manufacturing of geopolymer for sustainable built environment. *J Clean Prod* 2018;167. <https://doi.org/10.1016/j.jclepro.2017.08.165>.
- [127] Sun C, Xiang J, Xu M, He Y, Tong Z, Cui X. 3D extrusion free forming of geopolymer composites: materials modification and processing optimization. *J Clean Prod* 2020;258:120986. <https://doi.org/10.1016/j.jclepro.2020.120986>.
- [128] Xu Y, Šavija B. Development of strain hardening cementitious composite (SHCC) reinforced with 3D printed polymeric reinforcement: mechanical properties. *Compos B Eng* 2019;174. <https://doi.org/10.1016/j.compositesb.2019.107011>.
- [129] Salazar B, Aghdasi P, Williams ID, Ostertag CP, Taylor HK. Polymer lattice-reinforcement for enhancing ductility of concrete. *Mater Des* 2020;196:109184. <https://doi.org/10.1016/j.matdes.2020.109184>.
- [130] Cui Z. Printing practice for the fabrication of flexible and stretchable electronics. *Sci China Technol Sci* 2019;62:224–32. <https://doi.org/10.1007/s11431-018-9388-8>.
- [131] Jabari E, Ahmed F, Liravi F, Secor EB, Lin L, Toyserkani E. Two-dimensional printing of graphene: a review. *2D Mater* 2019.
- [132] Xu Y, Wu X, Guo X, Kong B, Zhang M, Qian X, et al. In: *The boom in 3D-printed sensor technology*, vol. 17; 2017. <https://doi.org/10.3390/s17051166>.
- [133] Yu X, Shou W, Mahajan BK, Huang X, Pan H. Materials, processes, and facile manufacturing for bioresorbable electronics: a review. *Adv Mater* 2018;30:1–27. <https://doi.org/10.1002/adma.201707624>.
- [134] Clower W, Hartmann MJ, Joffrion JB, Wilson CG. Additive manufactured graphene composite Sierpinski gasket tetrahedral antenna for wideband multi-frequency applications. *Addit Manuf* 2020;32. <https://doi.org/10.1016/j.addma.2019.101024>.
- [135] Zhang W, Wang H, Wang H, Chan JYE, Liu H, Zhang B, et al. Structural multi-colour invisible inks with submicron 4D printing of shape memory polymers. *Nat Commun* 2021;12. <https://doi.org/10.1038/s41467-020-20300-2>.
- [136] Elkholy A, Rouby M, Kempers R. Characterization of the anisotropic thermal conductivity of additively manufactured components by fused filament fabrication. *Prog Addit Manuf* 2019;4:497–515. <https://doi.org/10.1007/s40964-019-00098-2>.
- [137] van Grootel A, Chang J, Wardle BL, Olivetti E. Manufacturing variability drives significant environmental and economic impact: the case of carbon fiber reinforced polymer composites in the aerospace industry. *J Clean Prod* 2020;261:121087. <https://doi.org/10.1016/j.jclepro.2020.121087>.
- [138] Nickels L. AM and aerospace: an ideal combination. *Metal Powder Report* 2015;70. <https://doi.org/10.1016/j.mprp.2015.06.005>. Elsevier Ltd.
- [139] Najmon JC, Raeisi S, Tovar A. Review of additive manufacturing technologies and applications in the aerospace industry. Elsevier Inc.. 2019. <https://doi.org/10.1016/b978-0-12-814062-8.00002-9>.
- [140] Krueger H. Standardization for additive manufacturing in aerospace. *Engineering* 2017;3. <https://doi.org/10.1016/J.ENG.2017.05.010>. Elsevier LTD on behalf of Chinese Academy of Engineering and Higher Education Press Limited Company.
- [141] Han P. Additive design and manufacturing of jet engine parts. *Engineering* 2017;3:648–52. <https://doi.org/10.1016/J.ENG.2017.05.017>.
- [142] Klippstein H, Diaz De Cerio Sanchez A, Hassanin H, Zweiri Y, Seneviratne L. Fused deposition modeling for unmanned aerial vehicles (UAVs): a review. *Adv Eng Mater* 2018;20:1700552. <https://doi.org/10.1002/adem.201700552>.
- [143] Stratasys. World's first jet-powered, 3D printed UAV tops 150 mph with lightweight Stratasys materials [n.d].
- [144] Gardner JM, Sauti G, Kim JW, Cano RJ, Wincheski RA, Stelter CJ, et al. 3-D printing of multifunctional carbon nanotube yarn reinforced components. *Addit Manuf* 2016;12:38–44. <https://doi.org/10.1016/j.addma.2016.06.008>.
- [145] Saroia J, Wang Y, Wei Q, Lei M, Li X, Guo Y, et al. A review on 3D printed matrix polymer composites: its potential and future challenges. *Int J Adv Manuf Technol* 2020;106:1695–721. <https://doi.org/10.1007/s00170-019-04534-z>.
- [146] Lv X, Ye F, Cheng L, Fan S, Liu Y. Binder jetting of ceramics: powders, binders, printing parameters, equipment, and post-treatment. *Ceram Int* 2019;45:12609–24. <https://doi.org/10.1016/J.CERAMINT.2019.04.012>.
- [147] Cano S, Gooneie A, Kukla C, Rieb G, Holzer C, Gonzalez-Gutierrez J. Modification of interfacial interactions in ceramic-polymer nanocomposites by grafting: morphology and properties for powder injection molding and additive manufacturing. *Appl Sci* 2020;10. <https://doi.org/10.3390/app10041471>.
- [148] Karakoç A, Rastogi VK, Isoaho T, Tardy B, Paltakari J, Rojas OJ. Comparative screening of the structural and thermomechanical properties of FDM filaments comprising thermoplastics loaded with cellulose, carbon and glass fibers. *Materials (Basel)* 2020;13. <https://doi.org/10.3390/ma13020422>.
- [149] Bhandari S, Lopez-Anido RA, Gardner DJ. Enhancing the interlayer tensile strength of 3D printed short carbon fiber reinforced PETG and PLA composites via annealing. *Addit Manuf* 2019;30:100922. <https://doi.org/10.1016/j.addma.2019.100922>.
- [150] Joyee EB, Lu L, Pan Y. Analysis of mechanical behavior of 3D printed heterogeneous particle-polymer composites. *Compos B Eng* 2019;173. <https://doi.org/10.1016/j.compositesb.2019.05.051>.

**Ans Al Rashid** is a Ph.D. student at the Hamad Bin Khalifa University. Before joining HBKU, he obtained Master's degree in Mechanical Engineering from Politecnico Do Milano, Italy and Bachelors degree in Mechanical Engineering from University of Engineering and Technology Pakistan. His research focuses on experimental and numerical study of 3D printed polymer composites. He works on synthesis, 3D printing and mechanical and thermal characterization of these materials.

**Dr. Shoukat Alim Khan** is Postdoctoral researcher at Hamad bin khalifa university (HBKU), Qatar. He obtained his BS and MS degrees in Automotive and Mechanical engineering from Politecnico di Torino, Italy, and completed his Ph.D. degree in sustainable energy from HBKU. His research focus includes Thermal management of high power devices, Integrated renewable energy

systems, absorption cooling, micro-nano scale surfaces for energy applications, and 3D printing for built environment.

**Dr. Sami G. Al-Ghamdi** is an assistant professor of Sustainable Development, College of Science and Engineering at Hamad Bin Khalifa University (HBKU). He holds a PhD in Civil and Environmental Engineering from the University of Pittsburgh (2015), an MSc in Civil and Construction Engineering from Western Michigan University (2010) and a BSc in Architecture and Building Science from King Saud University (2005). Dr. Al-Ghamdi's work focuses on integrating life-cycle thinking using Life-Cycle Assessment (LCA) into policies and regulations related to green building. He is also working on energy efficiency measures in building design, construction, and operations processes. Specifically, in novel design processes that financially and technically facilitate energy-efficient buildings. Furthermore, he is interested in integrated project delivery systems and building information modeling (BIM).

**Dr. Muammer Koc** was appointed as a founding professor of sustainability at HBKU in 2014, Professor Koç held professor,

director, chair and dean positions at different universities in Turkey and the USA between 2000 and 2014. He has a PhD degree in Industrial and Systems Engineering from the Ohio State University (1999) and an Executive MBA degree from the University of Sheffield, UK (2014). He has published 130+ publications in various international journals and conferences; edited three books; organized, chaired, and co-chaired various international conferences, workshops and seminars on design, manufacturing and product development. In addition to his academic and educational activities, he provides consulting services to industry, government and educational institutes for strategic transformation, business optimization, organizational efficiency, lean operations, restructuring and reengineering initiatives. He has taught courses across a range of subjects, including product/process/business innovation and development; medical design and production; energy and efficiency; computer-aided engineering, design and manufacturing; modern manufacturing technologies; manufacturing system design; material forming plasticity; and the mechanical behavior of materials.